Brain-derived estrogens facilitate male-typical behaviors by potentiating androgen receptor signaling in medaka

Yuji Nishiike[1], Shizuku Maki[1], Daichi Miyazoe[1], Kiyoshi Nakasone[1], Yasuhiro Kamei[2], Takeshi Todo[3], Tomoko Ishikawa-Fujiwara[3], Kaoru Ohno[4], Takeshi Usami[4], Yoshitaka Nagahama[4], and Kataaki Okubo[1,*]

[1]Department of Aquatic Bioscience, Graduate School of Agricultural and Life Sciences, The University of Tokyo, Bunkyo, Tokyo 113-8657, Japan

[2]Optics and Bioimaging Facility, Trans-Scale Biology Center, National Institute for Basic Biology, Okazaki, Aichi 444-8585, Japan

[3]Department of Genome Biology, Graduate School of Medicine, Osaka University, Suita, Osaka 565-0871, Japan

[4]Division of Reproductive Biology, National Institute for Basic Biology, Okazaki, Aichi 444-8585, Japan

***Corresponding author:** Kataaki Okubo; Tel: +81-3-5841-5288. Fax: +81-3-5841-5289. E-mail: a-okubo@g.ecc.u-tokyo.ac.jp.

Abstract

In rodents, estrogens aromatized from androgens in the brain are essential for the development of male-typical behaviors. In many other vertebrates including humans and teleost fish, however, androgens facilitate these behaviors directly via the androgen receptor without aromatization into estrogens. Here we report that mutagenesis-derived male medaka fish lacking Cyp19a1b (a subtype of aromatase predominantly expressed in the brain) exhibit severely impaired male-typical mating and aggression, despite elevated brain androgen levels. These phenotypes can be rescued by estrogen administration, indicating that brain-derived estrogens are pivotal for male-typical behaviors even in teleosts. Our results further suggest that these estrogens facilitate male-typical behaviors by potentiating androgen action in the brain via the direct stimulation of androgen receptor transcription, thereby revealing a previously unappreciated mode of action of brain-derived estrogens. We additionally show that female fish lacking Cyp19a1b are less receptive to male courtship and conversely court other females, highlighting the significance of brain-derived estrogens in establishing sex-typical behaviors in both sexes.

Keywords: aggression; androgen receptor; aromatase; mating; brain-derived estrogens

Introduction

Male and female animals exhibit differences in many innate behaviors, such as mating and aggression (1). In vertebrates, these differences are driven primarily by the influence of sex steroid hormones, including estrogens and androgens. Extensive research in rodents has established that estrogens, traditionally considered "female" hormones, are critical for the development of male-typical behaviors (2–4). Specifically, androgens secreted by the testis, both perinatally and in adulthood, are converted to estrogens in the brain by the enzyme aromatase. These estrogens then act through ESR1, a subtype of the estrogen receptor (ESR), to elicit male-typical behaviors (2–4). This process, originally referred to as the "aromatization hypothesis", is now widely acknowledged; however, the mechanisms through which brain-derived estrogens affect male-typical behavior, including the identity of their downstream targets, remain largely elusive (4, 5).

More importantly, the aromatization hypothesis seems to apply to only a limited number of species besides rodents (e.g., some birds such as zebra finches) (6). In other species such as humans, other primates, and teleost fish, testicular androgens facilitate male-typical behaviors directly through the androgen receptor (AR) without aromatization (7–9). In primates, the hypothalamic aromatization of androgens to estrogens plays a central role in female gametogenesis (10) but is not essential for male behaviors (7, 8). Notably, in teleosts, 11-ketotestosterone (11KT), which cannot be aromatized to estrogens, is the primary testicular androgen, and exogenous 11KT effectively induces male-typical courtship and aggression even in females (9, 11, 12). Therefore, it is generally assumed that, in teleosts, androgens are largely responsible for male-typical behaviors, while estrogens are dispensable for these behaviors. This is consistent with recent observations in a few teleost species that genetic ablation of AR severely impairs male-typical behaviors (13–16) and with findings in medaka fish (*Oryzias latipes*) that estrogens act through the ESR subtype Esr2b to prevent females from engaging in male-typical courtship (12).

Interestingly, despite these findings, adult teleost brains have extremely high levels of aromatase activity (100–1000 times higher than in rodent brains), resulting in large amounts of brain estrogens even in males (17). In teleost brains, including those of medaka, aromatase is exclusively localized in radial glial cells, in contrast to its neuronal localization in rodent brains (18–20). These observations suggest that brain-derived estrogens have a vital, but as yet undetermined, role in male teleosts. It is worth mentioning that systemic administration of estrogens and an aromatase inhibitor increased and decreased male aggression, respectively, in several teleost species, potentially reflecting the behavioral effects of brain-derived estrogens (21–24). Most teleost species have two distinct genes encoding aromatase, *cyp19a1a* and *cyp19a1b*, due to a whole-genome duplication that occurred early in teleost evolution (17, 25). These genes have undergone subfunctionalization through the partitioning of tissue-specific expression patterns: *cyp19a1a* is expressed predominantly in the gonad, whereas *cyp19a1b* is expressed in the brain (17, 25). In medaka, *cyp19a1b* is also expressed in the gonads, but only at a level tens to hundreds of times lower than in the brain and substantially lower than that of *cyp19a1a* (26, 27).

In the present study, we generated *cyp19a1b*-deficient medaka, in which estrogen synthesis in the brain is selectively impaired while that in the gonads remains intact, in order to investigate the impact of brain-derived estrogens on male behaviors. Remarkably, the fish showed severely impaired male-typical behaviors, thus revealing the marked behavioral effects of these estrogens. Our results further suggest that these effects are mediated by potentiating androgen signaling in behaviorally relevant brain regions.

80 # Results

81

82 ### *cyp19a1b*-deficient males exhibit severely impaired male-typical mating and
83 aggressive behaviors

84 We generated a *cyp19a1b*-deficient medaka line from a mutant founder carrying a nonsense
85 mutation in exon 4 of *cyp19a1b* that was identified through screening of the medaka TILLING
86 (targeting-induced local lesions in genomes) library (28) (Fig. S1, A and B). Loss of *cyp19a1b* function
87 in these fish was verified by measuring brain and peripheral levels of sex steroids. As expected, brain
88 estradiol-17β (E2) in both male and female homozygous mutants (*cyp19a1b*$^{-/-}$) was significantly
89 reduced to 16% and 50%, respectively, of the levels in their wild-type (*cyp19a1b*$^{+/+}$) siblings ($P = 0.0037$,
90 males; $P = 0.0092$, females) (Fig. 1, A and B). In males, brain E2 in heterozygotes (*cyp19a1b*$^{+/-}$) was
91 also reduced to 45% of the level in wild-type siblings ($P = 0.0284$) (Fig. 1A), indicating a dosage effect
92 of *cyp19a1b* mutation. In contrast, peripheral E2 levels were unaltered in both *cyp19a1b*$^{-/-}$ males and
93 females (Fig. S1, C and D), consistent with the expected functioning of Cyp19a1b primarily in the brain.
94 Strikingly, brain levels of testosterone, as opposed to E2, increased 2.2-fold in *cyp19a1b*$^{-/-}$ males
95 relative to wild-type siblings ($P = 0.0006$) (Fig. 1A). Similarly, brain 11KT levels in *cyp19a1b*$^{-/-}$ males
96 and females increased 6.2- and 1.9-fold, respectively, versus wild-type siblings ($P = 0.0007$, males; $P =$
97 0.0316, females) (Fig. 1, A and B). These results show that *cyp19a1b*-deficient fish have reduced
98 estrogen levels coupled with increased androgen levels in the brain, confirming the loss of *cyp19a1b*
99 function. They also suggest that the majority of estrogens in the male brain and half of those in the
100 female brain are synthesized locally in the brain. In addition, peripheral 11KT levels in *cyp19a1b*$^{-/-}$
101 males and females increased 3.7- and 1.8-fold, respectively ($P = 0.0789$, males; $P = 0.0118$, females)
102 (Fig. S1, C and D), indicating peripheral influence in addition to central effects.

103 Next, we investigated the mating behavior of *cyp19a1b*-deficient males (Fig. 1C). The mating
104 behavior of medaka follows a stereotypical sequence. It begins with the male approaching and closely
105 following the female (following). The male then performs a courtship display, rapidly swimming in a
106 circular pattern in front of the female. If the female is receptive, the male grasps her with his fins
107 (wrapping), culminating in the simultaneous release of eggs and sperm (spawning) (16). Because 11KT,
108 the primary driver of male-typical behaviors in teleosts, was increased in *cyp19a1b*-deficient males, we
109 predicted that these fish would engage more actively in mating. Nevertheless, *cyp19a1b*$^{-/-}$ males showed
110 significantly longer latencies to initiate wrappings ($P = 0.0033$ versus *cyp19a1b*$^{+/+}$, $P = 0.0195$ versus
111 *cyp19a1b*$^{+/-}$) and to spawn ($P = 0.0051$ versus *cyp19a1b*$^{+/+}$, $P = 0.0195$ versus *cyp19a1b*$^{+/-}$) (Fig. 1D).
112 These results suggest that they are less motivated to mate, though an alternative interpretation that their
113 cognition or sexual preference may be altered cannot be dismissed.

114 However, no significant differences were evident in latencies to initiate followings and courtship
115 displays (Fig. 1D); therefore, the possibility that *cyp19a1b*-deficient males are less sexually attractive
116 and less preferred by females could not be ruled out. To ascertain whether *cyp19a1b*-deficient males are
117 indeed less motivated to mate, we further tested their mating behavior using *esr2b*-deficient females,

118 which are unreceptive to male courtship (12), as stimulus females (Fig. 1E); this test eliminates the
119 influence of female receptivity, facilitating an exclusive evaluation of male motivation to mate with
120 females (16). We found that *cyp19a1b*$^{-/-}$ males showed significantly longer latencies to initiate
121 followings (P = 0.0129 versus *cyp19a1b*$^{+/+}$, P = 0.0060 versus *cyp19a1b*$^{+/-}$), courtship displays (P =
122 0.0003 versus *cyp19a1b*$^{+/+}$, P = 0.0006 versus *cyp19a1b*$^{+/-}$), and wrapping attempts (P = 0.0009 versus
123 *cyp19a1b*$^{+/+}$, P = 0.0282 versus *cyp19a1b*$^{+/-}$) (Fig. 1F). In addition, they exhibited significantly fewer
124 courtship displays (P < 0.0001 versus both *cyp19a1b*$^{+/+}$ and *cyp19a1b*$^{+/-}$) and wrapping attempts (P <
125 0.0001 versus both *cyp19a1b*$^{+/+}$ and *cyp19a1b*$^{+/-}$) (Fig. 1G). These results thus confirmed that *cyp19a1b*-
126 deficient males are less motivated to mate. In our previous study, we found that *esr2b*-deficient females
127 court females preferentially over males (12). Consistent with that finding, here we observed that 12 of
128 15 *cyp19a1b*$^{+/+}$ females received courtship displays from the *esr2b*-deficient female, as compared with
129 only 2 of 15 *cyp19a1b*$^{+/+}$ males (P = 0.0003) (Fig. 1H). Curiously, we further observed that 8 of 15
130 *cyp19a1b*$^{-/-}$ males received courtship displays from the *esr2b*-deficient female (P = 0.0321 versus
131 *cyp19a1b*$^{+/+}$ males) (Fig. 1H). Perhaps *cyp19a1b*$^{-/-}$ males are misidentified as females by *esr2b*-deficient
132 females because they are reluctant to court or they exhibit some female-like behavior.
133 Next, we examined the intrasexual aggressive behavior of *cyp19a1b*-deficient males (Fig. 1I). The
134 aggressive behavior of teleosts including medaka consists of five types of behavioral acts: chases, fin
135 displays, circles, strikes, and bites (29). *cyp19a1b*$^{-/-}$ males exhibited all of these aggressive acts less
136 frequently than *cyp19a1b*$^{+/+}$ and/or *cyp19a1b*$^{+/-}$ males, with significant differences observed for chases
137 (P = 0.0123 versus *cyp19a1b*$^{+/-}$), fin displays (P = 0.0214 versus *cyp19a1b*$^{+/+}$), and bites (P = 0.0015
138 versus *cyp19a1b*$^{+/+}$, P = 0.0002 versus *cyp19a1b*$^{+/-}$) (Fig. 1J). These observations demonstrate that
139 *cyp19a1b*-deficient males are less aggressive toward other males.
140 In tilapia (*Oreochromis niloticus*), depletion of *cyp19a1b* has been reported to cause male infertility
141 due to efferent duct obstruction (30). If this is also the case in medaka, the observed behavioral defects
142 might be secondary to infertility, possibly due to the perception of impaired sperm release. We therefore
143 investigated the fertilization and hatching success of embryos derived from mating between *cyp19a1b*$^{-/-}$
144 males and wild-type females. Their fertilization and hatching rates were 88.5% (n = 183) and 93.2% (n
145 = 162), respectively, indicating that *cyp19a1b*-deficient male medaka have normal fertility.
146

147 **Brain-derived estrogens facilitate male-typical behaviors probably by stimulating brain**
148 **AR expression**

149 We considered that the impaired male-typical behaviors of *cyp19a1b*-deficient males might be
150 reasonably attributed to either reduced E2 or increased 11KT in the brain. The latter possibility seemed
151 unlikely because 11KT/AR signaling strongly promotes male-typical behaviors in teleosts (9, 13–16);
152 therefore, we tested the former possibility by examining whether E2 treatment would rescue the
153 behavioral phenotypes of *cyp19a1b*-deficient males (Fig. 2A). E2 treatment, while having no effect in
154 *cyp19a1b*$^{+/+}$ males (Fig. 2, B and C), significantly shortened the latency to (P = 0.0005) and increased
155 the number of (P = 0.0006) courtship displays in *cyp19a1b*$^{-/-}$ males (Fig. 2, D and E). These results

156 suggest that reduced E2 in the brain is the primary cause of the mating defects, highlighting a pivotal
157 role of brain-derived estrogens in male mating behavior. However, caution is warranted, as an indirect
158 peripheral effect of bath-immersed E2 on behavior cannot be ruled out, although this is unlikely given
159 the comparable peripheral E2 levels in *cyp19a1b*-deficient and wild-type males. In contrast to mating,
160 E2 treatment was not effective in restoring aggression in *cyp19a1b*$^{-/-}$ males (Fig. S2A). It is possible
161 that the treatment protocol used may have failed to replicate the estrogenic milieu necessary to induce
162 aggression in males.

163 We then considered the mechanism by which brain-derived estrogens facilitate male-typical
164 behaviors. Our previous study showed that exogenous E2 upregulates the expression of a subtype of AR,
165 Ara, in the medaka brain (31; note that Ara was termed Arb in this reference). We therefore hypothesized
166 that brain-derived estrogens may facilitate male-typical behaviors by stimulating Ara expression and
167 thereby potentiating 11KT/Ara signaling in the brain. To test this hypothesis, we first examined *ara*
168 expression in the brain of *cyp19a1b*-deficient males by in situ hybridization analysis. Expression of *ara*
169 was significantly lower in *cyp19a1b*$^{-/-}$ males than in *cyp19a1b*$^{+/+}$ males in several preoptic and
170 hypothalamic nuclei that are activated upon mating and/or attack in males (15), including the PPa, pPPp,
171 and NVT ($P = 0.0134$, 0.0372, and 0.0008, respectively) (Fig. 2, F and G; see Table S1 for abbreviations
172 of brain nuclei). We then performed a similar analysis for the other AR subtype, Arb. Expression of *arb*
173 was significantly lower in *cyp19a1b*$^{-/-}$ than in *cyp19a1b*$^{+/+}$ males in other preoptic and hypothalamic
174 nuclei activated upon mating and/or attack (16), including the PMp, aPPp, and NPT ($P = 0.0009$, 0.0413,
175 and 0.0021, respectively) (Fig. 2, H and I).

176 Next, to determine whether these reductions in *ara* and *arb* expression in *cyp19a1b*$^{-/-}$ males were
177 the result of reduced brain E2, we tested whether E2 treatment could restore the expression of the two
178 genes. In situ hybridization revealed significantly increased *ara* and *arb* expression in most brain nuclei
179 of E2-treated *cyp19a1b*$^{-/-}$ males as compared with vehicle-treated *cyp19a1b*$^{-/-}$ males (similar results
180 were obtained in *cyp19a1b*$^{+/+}$ males) (Fig. 2, J and K; Fig. S2, B and C; Fig. S3), indicating that the
181 decreased *ara* and *arb* expression in *cyp19a1b*$^{-/-}$ males is attributable to reduced E2 levels. Taken
182 together, these results suggest that brain-derived estrogens elicit male-typical behaviors by stimulating
183 *ara* and *arb* expression in behaviorally relevant brain regions.

184

185 **_cyp19a1b_ deficiency impairs behaviorally relevant signaling pathways downstream of**
186 **ARs**

187 We considered that, if our hypothesis that brain-derived estrogens facilitate male-typical behaviors
188 by potentiating androgen/AR signaling is correct, then *cyp19a1b*-deficient males should have impaired
189 activation of behaviorally relevant genes that act downstream of ARs. Two neuropeptide genes, *vt*
190 (encoding vasotocin) and *gal* (encoding galanin), have been implicated in male-typical mating and
191 aggressive behaviors in various vertebrates, including medaka and other teleosts (11, 16, 29, 32, 33). In
192 medaka, subsets of neurons in the pNVT and pPMp express *vt* and *gal*, respectively, in an androgen-
193 dependent and hence male-biased manner, and these neurons have been implicated in male-typical

194 behaviors (11, 29, 34). We therefore studied the expression of *vt* and *gal* in the brains of *cyp19a1b*-
195 deficient males.
196 In situ hybridization revealed that, as expected, expression of *vt* in the pNVT of *cyp19a1b*$^{-/-}$ males
197 was significantly reduced to 18% as compared with *cyp19a1b*$^{+/+}$ males ($P = 0.0040$), a level comparable
198 to that observed in females (Fig. 3, A and B). In contrast, there were no significant differences between
199 genotypes in other brain nuclei (Fig. 3A). Similarly, expression of *gal* in the pPMp of *cyp19a1b*$^{-/-}$ males
200 was reduced to 43% as compared with *cyp19a1b*$^{+/+}$ males ($P = 0.0019$), while no significant differences
201 were observed in other brain nuclei (Fig. 3, C and D). These results demonstrate that *cyp19a1b*
202 deficiency severely impairs the AR-dependent activation of behaviorally relevant *vt* and *gal* expression,
203 suggesting that brain-derived estrogens play a substantial role in activating AR signaling.
204
205 **Estrogens directly stimulate the transcription of ARs through ESRs**
206 The above results led us to further explore how brain-derived estrogens stimulate the expression of
207 *ara* and *arb*. In silico analysis of the medaka *ara* and *arb* loci identified two canonical bipartite estrogen-
208 responsive element (ERE)-like sequences in introns 1 and 2 of *ara* (located at positions +1699 and
209 +2050, respectively, relative to the transcription initiation site) and three in the 5′-flanking region of *arb*
210 (at positions –1272, –2180, and –3327) (Fig. 4, A and B). Thus, brain estrogens might be able to directly
211 activate the transcription of *ara* and *arb*. To evaluate this likelihood, we conducted in vitro
212 transcriptional activity assays in which luciferase expression was driven by genomic fragments from the
213 *ara* and *arb* loci containing the identified ERE-like sequences.
214 An assay using the *ara* genomic fragment revealed that E2 dose-dependently increased luciferase
215 activity in the presence of any ESR subtype (Esr1, Esr2a, or Esr2b) (Fig. 4C), suggesting that E2 has
216 the ability to directly activate *ara* transcription through ESRs. The introduction of a point mutation into
217 the ERE-like sequence at position +2050 abolished the E2-induced luciferase activity in the presence of
218 any ESR subtype, while mutation at +1699 had no such effect (Fig. 4D). These results suggest that the
219 ERE at position +2050 is responsible for E2-induced activation of *ara* transcription. Because there is
220 evidence that a single ERE half-site is sufficient to confer E2 responsiveness on several genes (35), we
221 performed the assay using *ara* genomic fragments in which a mutation was introduced in either half-site
222 of the ERE at +2050. E2 induction of luciferase activity was abrogated in both cases (Fig. S4A),
223 suggesting that both ERE half-sites are required to confer estrogen responsiveness on *ara*.
224 In the assay using the *arb* genomic fragment, E2 also dose-dependently increased luciferase activity
225 in the presence of any ESR subtype (Fig. 4E). The E2-induced increase was completely abolished by
226 point mutation of the ERE-like sequence at position –3327 in the presence of any ESR subtype (Fig.
227 4F). A similar effect was observed for mutation of the ERE-like sequence at position –1272, but only in
228 the presence of Esr1 and not in the presence of Esr2a or Esr2b (Fig. 4F). These results indicate that E2
229 can directly stimulate *arb* transcription, primarily through the ERE at –3327. Mutations in either half-
230 site of this ERE eliminated induction by E2 in the presence of Esr2a or Esr2b, but not Esr1 (Fig. S4B),
231 suggesting that both ERE half-sites are required to confer estrogen responsiveness on *arb*. Collectively,

these experiments suggest that the transcription of *ara* and *arb* can be directly stimulated by estrogens (including brain-derived estrogens) via the binding of ESRs to canonical bipartite EREs.

Brain-derived estrogens stimulate *ara* and *arb* expression in behaviorally relevant brain regions primarily through Esr2a and Esr1, respectively

Next, we investigated whether brain-derived estrogens can induce *ara* and *arb* expression through ESRs in vivo and, if so, which ESR subtype (Esr1, Esr2a, or Esr2b) mediates this induction. To this end, we examined *ara* and *arb* expression in the brains of males deficient for each ESR subtype by in situ hybridization. We used previously described *esr1*- and *esr2b*-deficient medaka (12, 36) and generated *esr2a*-deficient medaka using the CRISPR (clustered regularly interspaced short palindromic repeats) / Cas9 (CRISPR-associated protein 9) system. Two independent *esr2a*-deficient lines (Δ8 and Δ4) were established (Fig. S5) and used for subsequent behavioral experiments to ensure the reproducibility of the observed phenotypes.

In $esr1^{+/+}$ and $esr1^{-/-}$ males, *ara* expression was not significantly different between genotypes in any brain nucleus (Fig. S6A), but *arb* expression was significantly lower in $esr1^{-/-}$ than in $esr1^{+/+}$ males in the PMp and aPPp (P = 0.0111 and 0.0376, respectively) (Fig. 5, A and B). This, together with our observation that *arb* expression in these brain nuclei was also significantly lower in $cyp19a1b^{-/-}$ males (Fig. 2H), suggests that brain-derived estrogens stimulate *arb* expression in these nuclei primarily through Esr1. In support of this notion, double-label in situ hybridization in the wild-type male brain detected neurons coexpressing *arb* and *esr1* in both the PMp and aPPp (Fig. S6B). In $esr2a^{+/+}$ and $esr2a^{-/-}$ male brains (from the Δ8 line), *ara* expression was significantly lower in $esr2a^{-/-}$ than in $esr2a^{+/+}$ males in the PPa, pPPp, and NVT (P = 0.0359, 0.0430, and 0.0178, respectively) (Fig. 5, C and D), while no significant difference was observed in *arb* expression (Fig. S6C). Considering that *ara* expression in these nuclei was also lower in $cyp19a1b^{-/-}$ males (Fig. 2F), brain-derived estrogens presumably stimulate *ara* expression in these nuclei mainly through Esr2a. This idea was further supported by double-label in situ hybridization, which detected neurons coexpressing *ara* and *esr2a* in the PPa, pPPp, and NVT of wild-type males (Fig. S6D). Examination of $esr2b^{+/+}$ and $esr2b^{-/-}$ male brains showed significantly lower expression of *ara* in the NAT and higher expression of *arb* in the PPa of $esr2b^{-/-}$ males (Fig. S6, E to H); however, no such changes in expression were observed in $cyp19a1b^{-/-}$ males (Fig. 2, F and H). It therefore seems unlikely that Esr2b mediates the effect of brain estrogens on AR expression. Collectively, these results suggest that brain-derived estrogens stimulate *ara* and *arb* expression in behaviorally relevant brain regions primarily through Esr2a and Esr1, respectively.

esr1- and *esr2a*-deficient males are, respectively, less motivated to mate and less aggressive

If Esr1 and Esr2a truly mediate the behavioral effects of brain-derived estrogens through the activation of AR expression, then *esr1*- and *esr2a*-deficient males should exhibit impaired male-typical behaviors. More specifically, given that Esr1 and Esr2a function to activate the expression of *arb* and

270 *ara*, which are responsible for male mating and aggression, respectively (16), *esr1*- and *esr2a*-deficient
271 males should be less motivated to mate and less aggressive, respectively.
272 To test these ideas, we first evaluated the mating behavior of *esr1*-deficient males using a wild-type
273 female as the stimulus. As expected, *esr1*$^{-/-}$ males showed a significantly longer latency to initiate
274 followings than *esr1*$^{+/+}$ males (P = 0.0055) (Fig. S7), suggesting that they are less motivated to mate.
275 This was further confirmed in tests using an *esr2b*-deficient female as the stimulus, where *esr1*$^{-/-}$ males
276 showed a longer latency to followings and fewer courtship displays than *esr1*$^{+/+}$ males (P = 0.0426 and
277 0.0039, respectively) (Fig. 5, E to G). In contrast, no deficits were observed in the mating behavior of
278 *esr2a*$^{-/-}$ males toward wild-type females (Fig. S8, A and B). Although *esr2a*$^{-/-}$ males of the Δ8 line
279 showed a shorter latency to followings than their wild-type siblings in tests using a stimulus *esr2b*-
280 deficient female (P = 0.0146) (Fig. 5, H to J), this was not reproduced in the Δ4 line (Fig. S8, C and D).
281 We subsequently assessed aggressive behavior and found no defects in *esr1*$^{-/-}$ males (Fig. 5K).
282 Conversely, *esr2a*$^{-/-}$ males from both the Δ8 and Δ4 lines exhibited significantly fewer fin displays than
283 their wild-type siblings (P = 0.0461 and 0.0293, respectively). Circles followed a similar pattern, with
284 a significant reduction in the Δ8 line (P = 0.0446) and a comparable but non-significant decrease in the
285 Δ4 line (P = 0.1512) (Fig. 5L; Fig. S8E), showing less aggression. Taken together with the previous
286 finding that *esr2b*-deficient males show no deficits in either mating or aggressive behavior (12), these
287 results suggest that brain-derived estrogens can promote mating with females by stimulating *arb*
288 expression through Esr1 and can increase aggression toward other males by stimulating *ara* expression
289 through Esr2a. Nonetheless, behavioral deficits in *esr1*- and *esr2a*-deficient males were relatively mild
290 as compared with *cyp19a1b*-deficient males (Fig. 1) and *ara*- and *arb*-deficient males (16), suggesting
291 that a compensatory mechanism may exist between ESR subtypes.
292

293 **_cyp19a1b_-deficient females are less receptive to males and instead court other**
294 **females**

295 Finally, we tested the behavioral impact of *cyp19a1b* deficiency in females. Tests of the mating
296 behavior of *cyp19a1b*$^{-/-}$ females revealed that they had significantly longer latencies to receive the first
297 wrapping from the stimulus male (P = 0.0018 versus *cyp19a1b*$^{+/+}$, P = 0.0117 versus *cyp19a1b*$^{+/-}$) and
298 to spawn (P = 0.0015 versus *cyp19a1b*$^{+/+}$) (Fig. 6, A and B). These results are consistent with a recent
299 study in zebrafish (*Danio rerio*) showing that *cyp19a1b*-deficient females are less receptive to male
300 courtship (37). We further found that the number of courtship displays and wrapping attempts from the
301 male was not increased in *cyp19a1b*$^{-/-}$ females (Fig. 6C), despite their reduced receptivity. This suggests
302 that they are not only less receptive to male courtship but may also actively avoid males, depriving them
303 of mating opportunities. We tested this assumption by measuring the distance between fish, which
304 confirmed that *cyp19a1b*$^{-/-}$ females spent significantly less time near males at distances of 10–20 mm
305 (P = 0.0438) and 20–30 mm (P = 0.0002) as compared with *cyp19a1b*$^{+/+}$ females (Fig. 6D). We therefore
306 explored the possibility that *cyp19a1b*$^{-/-}$ females may develop a stronger sexual preference for females
307 than for males. In tests of the mating behavior between two females, 4 of 10 *cyp19a1b*$^{-/-}$ females

308 exhibited courtship displays toward the stimulus female, while 0 of 9 *cyp19a1b*$^{+/+}$ females did (P =
309 0.0396) (Fig. 6, E and F). These results demonstrate that *cyp19a1b*-deficient females, having a slightly
310 female-oriented sexual preference, are less receptive to male courtship and, conversely, court other
311 females.

312 Notably, these behavioral phenotypes of *cyp19a1b*-deficient females, albeit milder, closely resemble
313 those of *esr2b*-deficient females (12). This led us to hypothesize that *cyp19a1b* deficiency prevents
314 female-typical, and induces male-typical, behavioral phenotypes by decreasing estrogen/Esr2b signaling.
315 If correct, *cyp19a1b*-deficient females should be defective in the activation of behaviorally relevant
316 genes that act downstream of Esr2b. In medaka, subsets of neurons in the Vs/Vp and PMm/PMg express
317 *npba* (encoding neuropeptide B) in an estrogen/Esr2b signaling-dependent and hence female-specific
318 manner, and these neurons have been implicated in female sexual receptivity (12, 38, 39). We therefore
319 examined the expression of *npba* in the brains of *cyp19a1b*-deficient females by in situ hybridization.
320 As expected, *npba* expression in the Vs/Vp and PMm/PMg of *cyp19a1b*$^{-/-}$ females was significantly
321 reduced to 33% and 38%, respectively, of that of *cyp19a1b*$^{+/+}$ females (Vs/Vp, P = 0.0386; PMm/PMg,
322 P = 0.0461) (Fig. 6, G to J). Expression of *esr2b* in these brain nuclei is also estrogen-dependent and
323 female-specific (12, 31); therefore, we tested whether it is also attributable to brain-derived estrogens.
324 In situ hybridization showed no significant differences in *esr2b* expression between *cyp19a1b*$^{+/+}$ and
325 *cyp19a1b*$^{-/-}$ females in the Vs/Vp and PMm/PMg, although significant differences were seen in the VM,
326 NAT, and NVT (Fig. 6K), suggesting that *esr2b* expression in the brain relies on ovarian estrogens and
327 not on brain-derived estrogens. Taken altogether, our findings indicate that brain-derived estrogens
328 contribute substantially to the induction of female-typical, and the prevention of male-typical, behaviors
329 in females by activating estrogen/Esr2b signaling.

Discussion

In this study, we found that male medaka deficient for *cyp19a1b* exhibit severely impaired male-typical mating and aggression. This observation was noteworthy because the fish had markedly elevated brain levels of 11KT, the primary driver of male-typical behaviors in teleosts (9, 11). Deficits in mating were rescued by estrogen administration, indicating that reduced brain estrogen levels are the primary cause of the observed mating impairment; in other words, brain-derived estrogens are pivotal at least for male-typical mating behaviors in teleosts. This was also notable because, unlike in rodents, where the necessity for brain-derived estrogens has been codified as the "aromatization hypothesis", these estrogens have been regarded as dispensable for male behaviors in many vertebrates, including teleosts (7–9). In addition, the rescue of behavioral phenotypes by estrogen administration in adults suggests that in teleosts, unlike in rodents, brain-derived estrogens early in life is not essential for the execution of male-typical behaviors. While brain-derived estrogens are necessary for male behaviors in both rodents and teleosts, the life stages at which they exert their behavioral effects probably differ between these species. Brain aromatase activity in teleosts increases with age and, at adulthood, reaches 100–1000 times that in rodents (9, 17). In contrast, brain aromatase activity in rodents reaches its peak during the perinatal period and thereafter declines with age (40), although it remains important for male behavior in adulthood. This variation among species may represent the activation of brain estrogen synthesis at life stages critical for sexual differentiation of behavior that are unique to each species.

Brain-derived estrogens serve several functions during the process of sexual differentiation of the mouse brain, including the synthesis of prostaglandin PGE2 and the activation of synaptic and neurodevelopmental genes; however, the specific mechanism whereby these estrogens affect male behaviors remains obscure (4, 5, 41). Our findings in medaka indicate that brain-derived estrogens facilitate male-typical behaviors by potentiating androgen/AR signaling in behaviorally relevant brain regions via the direct stimulation of AR transcription. More specifically, they indicate that brain-derived estrogens (1) promote mating by stimulating the transcription of *arb* in some preoptic and hypothalamus nuclei via Esr1, and (2) increase aggression by stimulating the transcription of *ara* in other preoptic and hypothalamus nuclei through Esr2a. This model of the mechanism underlying the action of brain-derived estrogens would explain the apparent contradiction that, in teleosts, androgens per se elicit male behaviors without aromatization, while estrogen synthesis in the brain are also critical for these behaviors. Our data also indicate that the two AR genes, *ara* and *arb*, are direct downstream targets of brain-derived estrogens that mediate male behaviors, only a few of which have been identified thus far. In mice, perinatal brain estrogens increase *Ar* expression in the bed nucleus of the stria terminalis and preoptic area, two brain regions that have been implicated in male behaviors (42). Recent evidence suggests that ESR1 binds to the regulatory genomic region of *Ar* in these brain regions in mice (41). Given these facts, the idea that brain-derived estrogens enhance androgen/AR signaling by directly stimulating AR transcription may apply to a wide range of species, including rodents.

Consistent with our results, studies in several teleost species have shown that treatment of males

368 with an aromatase inhibitor reduces their male-typical behaviors, while estrogens exert the opposite
369 effect (21–24). Conversely, it has been shown in various teleosts, including medaka, that treatment with
370 exogenous estrogens attenuates male behaviors (43–47). A possible explanation for this discrepancy is
371 that estrogens may either stimulate or suppress male-typical behaviors, depending on their concentration.
372 All studies showing the suppressive effects of exogenous estrogens were conducted at doses higher than
373 those used in the present study or at doses mimicking the levels typical of adult females (48). In addition,
374 our previous study in male medaka showed that high doses of exogenous estrogens induce the expression
375 of *esr2b*, which prevents male-typical mating behavior, in behaviorally relevant brain regions (12). Thus,
376 the development of male behaviors may require moderate brain estrogen levels that are sufficient to
377 induce the expression of *ara* and *arb*, but not *esr2b*, in the underlying neural circuitry. This may account
378 for the lack of aggression recovery in E2-treated *cyp19a1b*-deficient males in this study. Another
379 possibility that is not mutually exclusive is that endogenous levels of brain estrogens are sufficient to
380 motivate males to engage in male-typical behaviors, and therefore exogenous estrogens have no further
381 effect. This possibility is at least likely for mating behavior, as estrogen treatment facilitated mating
382 behavior in *cyp19a1b*-deficient males but not in their wild-type siblings. Further studies using *cyp19a1b*
383 mutants from different teleost species are needed to explore these possibilities and to determine whether
384 the findings in medaka hold for other teleosts.
385 We also found that, as compared with males, females have higher brain levels of estrogens, with half
386 being synthesized locally and the other half supplied by the ovaries. In many brain nuclei of medaka,
387 expression of *ara* and *arb* is comparable between the sexes or at higher levels in females (31), suggesting
388 that brain-derived estrogens stimulate AR expression in females as well as in males. This raises the issue
389 of why females do not display male-typical behaviors despite such high brain levels of estrogens and
390 active estrogen synthesis in the brain. Possibly, as mentioned above, high estrogen levels in the female
391 brain may suppress male-typical behaviors by promoting the expression of *esr2b*. Another possibility is
392 that females, despite having abundant ARs in the brain, may lack sufficient amounts of androgen to
393 activate them. This seems highly probable because the treatment of female medaka and other teleosts
394 with 11KT as adults readily induces male-typical behaviors, including courtship and aggression (9, 11,
395 12).
396 We found that *cyp19a1b*-deficient females are less receptive to male courtship, demonstrating that
397 brain-derived estrogens influence female, as well as male, mating behavior. This finding is notable when
398 considering that, contrary to mammals and birds, estrogens have been deemed unnecessary for female
399 sexual receptivity in teleosts (49). This notion essentially stems from the observation in several teleost
400 species that exogenous prostaglandin PGF2α is sufficient to restore sexual receptivity in females
401 deprived of ovarian secretions by ovariectomy (50–52). However, we recently challenged it by showing
402 that female medaka deficient for *esr2b* are completely unreceptive to males, and thus estrogens play a
403 critical role in female receptivity (12). Given that estrogen/Esr2b signaling feminizes the neural
404 substrates that mediate mating behavior, while PGF2α signaling triggers female sexual receptivity, the
405 present finding provides a likely explanation for this apparent contradiction, namely, that brain-derived

406 estrogens, rather than or in addition to ovarian-derived circulating estrogens, may function upstream of
407 PGF2α signaling to mediate female receptivity. This scheme potentially applies to other teleost species
408 because a reduction in female receptivity due to *cyp19a1b* deficiency has been also observed in zebrafish
409 (37).

410 We further found that *cyp19a1b*-deficient females court other females. To our knowledge, only a
411 few neuronal genes have been identified whose depletion causes females to display male-typical
412 behaviors in vertebrates. These include *trpc2* (encoding a cation channel crucial for olfactory cue-
413 evoked signaling in the vomeronasal organ) and *dmnt3a* (encoding a methyltransferase responsible for
414 de novo DNA methylation) in mice, and *esr2b* in medaka (12, 53, 54). Importantly, deficiency of
415 *cyp19a1b*, unlike that of *esr2b*, did not completely preclude female-typical mating behavior in females,
416 but caused them to exhibit both male- and female-typical mating behaviors. This observation suggests
417 that, in teleosts, the neural circuits mediating these behaviors coexist in the female brain and may be
418 activated simultaneously in the absence of brain estrogens. This probably also holds true for the male
419 brain, given that *cyp19a1b*-deficient males also showed impaired, but not completely abolished, male-
420 typical behaviors and were actively courted by *esr2b*-deficient females. It is thus plausible that brain-
421 derived estrogens are required to prevent the simultaneous activation of neural circuits mediating male-
422 and female-typical behaviors, thereby contributing to the mutually exclusive presentation of these
423 behaviors. Such effects of brain estrogens are likely to be particularly relevant in teleosts, where many
424 species spontaneously undergo sex reversal and their sexual phenotypes, behavioral or otherwise, are
425 highly labile throughout life (55, 56). This may account for the extremely high levels of aromatase
426 activity in the teleost brain.

427 In summary, we have shown that brain-derived estrogens promote male-typical behaviors by
428 increasing brain sensitivity to testicular androgens through the stimulation of AR expression. Our
429 findings challenge the prevailing view that brain-derived estrogens have little effect on male-typical
430 behaviors in species where testicular androgens elicit these behaviors directly without aromatization to
431 estrogens in the brain and unveil a previously unappreciated mechanism of the action of brain-derived
432 estrogens. Because these species account for the majority of vertebrates, with rodents and some birds
433 being the only known exceptions, the mechanism of their action that we have identified in medaka may
434 be evolutionarily ancient and widely conserved across species.

435 # Materials and Methods

436

437 ## Animals and cell lines

438 Wild-type d-rR strain medaka and mutant medaka deficient for *cyp19a1b* and *esr2a* (generated in
439 this study), *esr1* (36), and *esr2b* (12) were maintained in a recirculating system at 28ºC on a 14/10-hour
440 light/dark cycle. Three or four times a day, they were fed live brine shrimp and dry food (Otohime;
441 Marubeni Nisshin Feed, Tokyo, Japan). Sexually mature adults (2–6 months) were used for experiments,
442 and tissues were consistently sampled 1–5 hours after lights on. In each experiment, siblings raised
443 under the same conditions were used as the comparison group to control for the effects of genetic
444 diversity and environmental variation. All fish were handled in accordance with the guidelines of the
445 Institutional Animal Care and Use Committee of the University of Tokyo.

446 HEK293T and HeLa cells used in this study were confirmed to be mycoplasma-free (Biotherapy
447 Institute of Japan, Tokyo, Japan) and authenticated by short tandem repeat profiling (National Institute
448 of Biomedical Innovation, Osaka, Japan).

449

450 ## Generation of mutant medaka

451 *cyp19a1b*-deficient medaka were generated essentially as previously described (12). In brief, a
452 TILLING library of 5760 chemically mutagenized medaka (28) was screened for mutations in exons 3,
453 4, and 5 of *cyp19a1b* by direct sequencing of PCR-amplified fragments. A founder (ID: 57D05) with a
454 nonsense mutation in exon 4 (K105*) was identified (Fig. S1, A and B) and backcrossed to the wild-
455 type d-rR strain for more than six generations to eliminate background mutations. Heterozygous males
456 and females were intercrossed to generate wild-type, heterozygous, and homozygous siblings. All
457 experimental fish were subjected to genotyping by PCR amplification across the mutation, followed by
458 high-resolution melting (HRM) analysis, using the primers and probe listed in Table S2. HRM analysis
459 was performed on the LightCycler 480 System II (Roche Diagnostics, Basel, Switzerland) using the
460 LCGreen Plus dye (BioFire Defense, Salt Lake City, UT).

461 *esr2a*-deficient medaka were generated by using the CRISPR/Cas9 system. A CRISPR RNA
462 (crRNA) targeting exon 3 of *esr2a* (Fasmac, Kanagawa, Japan) (Fig. S5A) was injected with trans-
463 activating crRNA (Fasmac) and Cas9 protein (Nippon Gene Co. Ltd., Tokyo, Japan) into the cytoplasm
464 of one- or two-cell stage embryos. The resulting fish were screened for germline mutations by
465 outcrossing to wild-type fish and testing progeny for target site mutations by T7 endonuclease I assay
466 (57) and direct sequencing. Two founders were identified that reproducibly yielded progeny carrying
467 frameshift mutations that eliminated the DNA- and ligand-binding domains of Esr2a: one yielded
468 progeny carrying an 8-bp deletion (Δ8); the other yielded progeny carrying a 4-bp deletion (Δ4) (Fig.
469 S5, A and B). The DNA- and ligand-binding domains of medaka Esr2a were identified by sequence
470 alignment with yellow perch (*Perca flavescens*) Esr2a, for which these domain locations have been
471 reported (58). The progeny were intercrossed to obtain wild-type, heterozygous, and homozygous
472 siblings. The genotype of each experimental fish was determined by HRM analysis as described above.

473 A previous study reported that *esr2a*-deficient female medaka cannot release eggs due to oviduct
474 atresia (59). Likewise, some *esr2a*-deficient females generated in this study, despite the limited sample
475 size, exhibited spawning behavior but were unable to release eggs (Δ8 line: 2/3; Δ4 line: 1/1), while
476 such failure was not observed in wild-type females (Δ8 line: 0/12; Δ4 line: 0/11). These results support
477 the effective loss of *esr2a* function.
478
479 **Measurement of sex steroid levels**
480 Brain and peripheral levels of sex steroids were determined by enzyme-linked immunosorbent assay
481 (ELISA) (12). Total lipids were extracted from the brain and peripheral tissues (from the caudal half) of
482 *cyp19a1b*$^{+/+}$, *cyp19a1b*$^{+/-}$, and *cyp19a1b*$^{-/-}$ males and females with chloroform/methanol (2:1, v/v) and
483 purified on a Sep-Pak C18 Plus Light Cartridge (Waters Corporation, Milford, MA). Tissue levels of
484 E2, testosterone, and 11KT were measured by using Estradiol, Testosterone, and 11-Keto Testosterone
485 ELISA kits, respectively (Cayman Chemical Company, Ann Arbor, MI).
486
487 **Mating behavior test**
488 Mating behavior was tested essentially as previously described (39). In brief, on the day before
489 behavioral testing, each focal fish (*cyp19a1b*-, *esr1*-, and *esr2a*-deficient lines) was placed with a
490 stimulus fish (wild-type females in the tests shown in Fig. 1, C and D, Fig. 6, E and F, Fig. S7, and Fig.
491 S8, A and B; *esr2b*-deficient females in Fig. 1, E to H, Fig. 2, A to E, Fig. 5, E to J, and Fig. S8, C and
492 D; wild-type males in Fig. 6, A to C) in a 2-liter rectangular tank with a perforated transparent partition
493 separating them. The set-up was modified for E2-treated males, which were kept on E2 treatment and
494 not introduced to the test tanks until the day of testing to ensure the efficacy of E2 treatment. The
495 partition was removed 1 hour after lights on, and fish were allowed to interact for 30 min while their
496 behavior was recorded with a digital video camera (HC-V360MS, HC-VX985M, or HC-W870M;
497 Panasonic Corporation, Osaka, Japan). The first 15 min of the recording was used to calculate the latency
498 to the first following, courtship display, wrapping, and spawning. The period of interaction/recording
499 was extended to 2 hours in tests of courtship displays received from the stimulus *esr2b*-deficient female
500 and in tests of mating behavior between females, because they take longer to initiate courtship (12). In
501 tests using an *esr2b*-deficient female as the stimulus fish, where the latency to spawn could not be
502 calculated because these fish were unreceptive to males and did not spawn, the sexual motivation of the
503 focal fish was instead assessed by counting the number of courtship displays and wrapping attempts in
504 30 min. The number of these mating acts was also counted in tests to evaluate the receptivity of females.
505 In tests of mating behavior between two females, the stimulus female was marked with a small notch in
506 the caudal fin to distinguish it from the focal female.
507
508 **Aggressive behavior test**
509 To test male–male aggressive behavior (29), four males of the same genotype (*cyp19a1b*-, *esr1*-,
510 and *esr2a*-deficient lines) that were unfamiliar with one another were placed together in a test tank 1

511 hour after lights on. After 1 min of acclimation to the tank, fish were allowed to interact for 15 min
512 while their behavior was video-recorded as described above. The total number of each aggressive act
513 (chase, fin display, circle, strike, and bite) displayed by the four males in the tank was counted manually
514 from the video recordings.
515
516 **E2 treatment**
517 *cyp19a1b*$^{+/+}$ and *cyp19a1b*$^{-/-}$ males were treated with 1 ng/ml of E2 (Fujifilm Wako Pure Chemical,
518 Osaka, Japan), which was first dissolved in 100% ethanol (vehicle), or with the vehicle alone by
519 immersion in water for 4 days, with daily water changes to maintain the nominal concentration. The
520 mating and aggressive behaviors of males before and after E2 treatment were evaluated as described
521 above. The expression of *ara* and *arb* in the brain of E2- and vehicle-treated males was investigated by
522 single-label in situ hybridization as described below. Although the exact increase in brain E2 levels
523 following E2 treatment was not quantified, the observed positive effects on behavior and gene
524 expression suggest that it was sufficient.
525
526 **Single-label in situ hybridization**
527 Digoxigenin (DIG)-labeled cRNA probes were generated by in vitro transcription using DIG RNA
528 Labeling Mix (Roche Diagnostics), T7 RNA polymerase (Roche Diagnostics), and the following cDNA
529 fragments: *ara*, nucleotide 16–1030 of GenBank NM_001122911 (1015 bp); *arb*, 53–1233 of
530 NM_001104681 (1181 bp); *vt*, 1–845 of NM_001278891 (845 bp); *gal*, 5–533 of LC532140 (529 bp);
531 *npba*, 1–645 of NM_001308979 (645 bp); and *esr2b*, 2080–3288 of XM_020713365 (1209 bp).
532 Single-label in situ hybridization was essentially done as described (60). In brief, brains dissected
533 from males and females of the *cyp19a1b*-deficient line (analysis of *ara*, *arb*, *vt*, *gal*, *npba*, and *esr2b*)
534 and males of the *esr1*-, *esr2a*-, and *esr2b*-deficient lines (analysis of *ara* and *arb*) were fixed in 4%
535 paraformaldehyde and embedded in paraffin. Serial coronal sections of 10-μm thickness were
536 hybridized with a DIG-labeled probe. Hybridization signal was detected with anti-DIG conjugated to
537 alkaline phosphatase (RRID: AB_514497; Roche Diagnostics) and visualized using 5-bromo-4-chloro-
538 3-indolyl phosphate/nitro blue tetrazolium substrate (Roche Diagnostics). After color development for
539 15 min (*gal*), 40 min (*npba*), 2 hours (*vt*), or overnight (*ara*, *arb*, and *esr2b*), sections were imaged using
540 a VS120 virtual slide microscope (Olympus, Tokyo, Japan). The total area of signal across all relevant
541 sections, including both hemispheres, was calculated for each brain nucleus using Olyvia software
542 (Olympus). Images were converted to a 256-level intensity scale, and pixels with intensities from 161
543 to 256 were considered signals. All sections used for comparison were processed in the same batch,
544 without corrections between samples. Medaka brain atlases (61, 62) were used to identify brain nuclei.
545
546 **Transcriptional activity assay**
547 Each full-length coding region of medaka Esr1 (GenBank XM_020714493), Esr2a
548 (NM_001104702), and Esr2b (XM_020713365) cDNA was amplified by PCR and inserted into the

549 expression vector pcDNA3.1/V5-His-TOPO (Thermo Fisher Scientific, Waltham, MA). Each
550 nucleotide sequence of the 5′-flanking region of *ara* and *arb* was retrieved from the Ensembl medaka
551 genome assembly and analyzed for potential canonical ERE-like sequences using Jaspar (version
552 5.0_alpha) and Match (public version 1.0) with default settings. No ERE-like sequence was detected in
553 *ara*; therefore, the gene body and 3′-flanking region were also analyzed in this case. The transcription
554 initiation site for *ara* and *arb* was determined based on an expressed sequence tag clone deposited in
555 National BioResource Project (NBRP) Medaka (olova36n18) and GenBank NM_001104681,
556 respectively. Medaka bacterial artificial chromosome (BAC) clones containing the *ara* (clone ID: ola1-
557 111G01) and *arb* (ola1-192H15) loci were obtained from NBRP Medaka. A 4530-bp genomic DNA
558 fragment upstream of *ara* exon 3 (comprising 2330 bp of the 5′-flanking region, exon 1, intron 1, exon
559 2, intron 2, and the first 32 bp of exon 3) was amplified by PCR from the BAC clone, fused to a P2A
560 self-cleaving peptide sequence (63) at the 3′ end, and inserted into the NheI site of the luciferase reporter
561 vector pGL4.10 (Promega, Madison, WI). Similarly, a 3995-bp fragment upstream of the first
562 methionine codon of *arb* (comprising 3815 bp of the 5′-flanking region and 180 bp of exon1) was PCR-
563 amplified and inserted into pGL4.10. The resulting constructs were transiently transfected into
564 HEK293T (*ara*) or HeLa (*arb*) cells, together with an internal control vector pGL4.74 (Promega) and
565 the Esr1, Esr2a, or Esr2b expression construct using Lipofectamine LTX (Thermo Fisher Scientific).
566 Six hours after transfection, cells were incubated for 18 hours without and with E2 at doses of 10^{-11} M,
567 10^{-9} M, and 10^{-7} M in Dulbecco's modified Eagle's medium (phenol red-free) containing 5%
568 charcoal/dextran-stripped fetal bovine serum (Cytiva, Marlborough, MA). Luciferase activity was
569 determined using the Dual-Luciferase Reporter Assay System (Promega) on the GloMax 20/20n
570 Luminometer (Promega). All assays were conducted in duplicate or triplicate and repeated
571 independently three times.
572 Further assays were performed with luciferase reporter constructs carrying point mutations in the
573 ERE-like sequences to identify the ERE responsible for E2 induction of *ara* and *arb* transcription. Each
574 half-site of the responsible ERE-like sequence was mutated into a HindIII recognition site using the
575 PrimeSTAR Mutagenesis Basal Kit (Takara Bio, Shiga, Japan). Transcriptional activity assays with
576 these constructs were done as described above, except that a single dose of E2 (10^{-7} M) was used.
577

578 **Double-label in situ hybridization**

579 DIG-labeled cRNA probes for *ara* and *arb* were prepared as described above. Fluorescein-labeled
580 cRNA probes for *esr1* and *esr2a* were generated by in vitro transcription using Fluorescein RNA
581 Labeling Mix (Roche Diagnostics), SP6 or T7 RNA polymerase (Roche Diagnostics), and the following
582 cDNA fragments: *esr1*, nucleotides 1694–2781 of XM_020714493 (1088 bp); *esr2a*, 1838–2276 of
583 NM_001104702 plus 763 bp of 3′-untranslated sequence derived from the Ensembl medaka genome
584 assembly (439 bp).
585 Double-label in situ hybridization was done as described previously (36), with minor modifications.
586 In brief, brains dissected from wild-type males were fixed in 4% paraformaldehyde, embedded in

587 paraffin, and coronally sectioned at 10-μm thickness. Sections were hybridized simultaneously with the
588 DIG-labeled *ara* or *arb* probe and fluorescein-labeled *esr1* or *esr2a* probe. DIG was detected with a
589 mouse anti-DIG antibody (RRID: AB_304362; Abcam, Cambridge, UK) and visualized using the Alexa
590 Fluor 555 Tyramide SuperBoost Kit, goat anti-mouse IgG (Thermo Fisher Scientific); fluorescein was
591 detected with an anti-fluorescein antibody conjugated to horseradish peroxidase (RRID: AB_2737388;
592 PerkinElmer, Waltham, MA) and visualized using the TSA Plus Fluorescein System (PerkinElmer).
593 Cell nuclei were counterstained with DAPI. Fluorescent images were acquired with a Leica TCS SP8
594 confocal laser scanning microscope (Leica Microsystems, Wetzlar, Germany) and the following
595 excitation/emission wavelengths: 552/620–700 nm (Alexa Fluor 555), 488/495–545 nm (fluorescein),
596 and 405/410–480 nm (DAPI). Cells were identified as coexpressing the two genes when Alexa Fluor
597 555 and fluorescein signals were clearly observed in the cytoplasm surrounding DAPI-stained nuclei,
598 with intensities markedly stronger than the background noise.
599
600 **Measurement of spatial distances between fish**
601 The distance between the two fish in the test tank was measured as described elsewhere (12). On the
602 day preceding measurement, each focal female (*cyp19a1b*-deficient line) and a stimulus wild-type male
603 were placed together in a 2-liter rectangular tank with a perforated transparent partition separating them.
604 On the following day after lights on, the fish were transferred to a 25-cm (i,d,) cylindrical test tank
605 containing 1.8 L of dechlorinated tap water with a transparent partition separating them. One hour after
606 lights on, the partition was removed and the behavior of the fish was video-recorded for 10 min.
607 Distances between fish were calculated by using UMA Tracker (64).
608
609 **Statistical analysis**
610 All quantitative data were expressed as mean ± standard error of the mean (SEM). On graphs,
611 individual data points were plotted to indicate the underlying distribution. Behavioral time-series data
612 were analyzed using Kaplan–Meier plots with the inclusion of fish that did not exhibit the given act
613 within the test period.
614 Statistical analyses were done using GraphPad Prism (GraphPad Software, San Diego, CA). Data
615 between two groups were compared using unpaired two-tailed Student's *t* test. Welch's correction was
616 applied if the *F* test indicated that the variance between groups was significantly different. The
617 Bonferroni–Dunn correction was applied for multiple comparisons between two groups. To compare
618 data among more than two groups, one-way analysis of variance (ANOVA) was performed, followed
619 by either Bonferroni's (comparisons among experimental groups) or Dunnett's (comparisons between
620 untreated and E2-treated groups in Fig. 4, C and D) post hoc test. If the Brown-Forsythe test indicated
621 a significant difference in variance across groups, the data were instead analyzed using the non-
622 parametric Kruskal–Wallis test, followed by Dunn's post hoc test. Differences between Kaplan–Meier
623 curves were tested for significance using the Gehan–Breslow–Wilcoxon test (with Bonferroni's
624 correction for more than two comparisons). Fish that spawned without any courtship display were

excluded from the analysis of courtship display because it was not appropriate to treat them either as fish that did not perform courtship displays within the test duration or as fish that performed the first courtship display 0 seconds before spawning. Specifically, 7/18 *cyp19a1b*$^{+/+}$, 11/18 *cyp19a1b*$^{+/-}$, and 6/18 *cyp19a1b*$^{-/-}$ males were excluded in Fig. 1D; 6/10 *cyp19a1b*$^{+/+}$, 3/10 *cyp19a1b*$^{+/-}$, and 6/10 *cyp19a1b*$^{-/-}$ females were excluded in Fig. 6B; 2/23 *esr1*$^{+/+}$ and 5/24 *esr1*$^{-/-}$ males were excluded in Fig. S7; 2/24 *esr2a*$^{+/+}$ and 3/23 *esr2a*$^{-/-}$ males were excluded in Fig. S8A; 0/23 *esr2a*$^{+/+}$ and 0/23 *esr2a*$^{-/-}$ males were excluded in Fig. S8B. All data points were included in the analyses and no outliers were defined.

Acknowledgments

We thank NBRP Medaka for providing the BAC clones, managing the TILLING library, and performing artificial insemination; Dr. Yoshihito Taniguchi for constructing the TILLING library; Dr. Masatoshi Nakamoto for recovering the *cyp19a1b* mutant allele; Akira Hirata, Kaoru Furukawa, Tomiko Iba, and Ayu Kuwakubo for assistance with medaka husbandry. This work was supported by the Ministry of Education, Culture, Sports, Science, and Technology (MEXT), Japan (17H06429 to KOk), the Japan Society for the Promotion of Science (JSPS) (21J20634 to YNi and 23H02305 to KOk), and Regional Fish Institute (Get-Research Grant to KOk).

References

1. N. Zilkha, Y. Sofer, Y. Kashash, T. Kimchi, The social network: neural control of sex differences in reproductive behaviors, motivation, and response to social isolation. *Curr. Opin. Neurobiol.* **68**, 137–151 (2021).
2. S. Ogawa, S. Tsukahara, E. Choleris, N. Vasudevan, Estrogenic regulation of social behavior and sexually dimorphic brain formation. *Neurosci. Biobehav. Rev.* **110**, 46–59 (2020).
3. S. Tsukahara, M. Morishita, Sexually dimorphic formation of the preoptic area and the bed nucleus of the stria terminalis by neuroestrogens. *Front. Neurosci.* **14**, 797 (2020).
4. M. M. McCarthy, Neural control of sexually dimorphic social behavior: connecting development to adulthood. *Annu. Rev. Neurosci.* **46**, 321–339 (2023).
5. M. M. McCarthy, B. M. Nugent, K. M. Lenz, Neuroimmunology and neuroepigenetics in the establishment of sex differences in the brain. *Nat. Rev. Neurosci.* **18**, 471–484 (2017).
6. J. Balthazart, New concepts in the study of the sexual differentiation and activation of reproductive behavior, a personal view. *Front. Neuroendocrinol.* **55**, 100785 (2019).
7. J. Thornton, J. L. Zehr, M. D. Loose, Effects of prenatal androgens on rhesus monkeys: a model system to explore the organizational hypothesis in primates. *Horm. Behav.* **55**, 633–645 (2009).
8. J. Bakker, The role of steroid hormones in the sexual differentiation of the human brain. *J. Neuroendocrinol.* **34**, e13050 (2022).
9. K. Okubo, Y. Nishiike, T. Fleming, Y. Kikuchi, T. Hiraki-Kajiyama, "Sex steroid regulation of male- and female-typical mating behaviors in teleost fish" in *Spectrum of Sex*, M. Tanaka, M. Tachibana, Eds. (Springer Nature, 2022), pp. 111–133.
10. E. Terasawa, Neuroestradiol in regulation of GnRH release. *Horm. Behav.* **104**, 138–145 (2018).
11. Y. Kawabata-Sakata, S. Kanda, K. Okubo, Male-specific vasotocin expression in the medaka tuberal hypothalamus: androgen dependence and probable role in aggression. *Mol. Cell. Endocrinol.* **580**, 112101 (2024).
12. Y. Nishiike, D. Miyazoe, R. Togawa, K. Yokoyama, K. Nakasone, M. Miyata, Y. Kikuchi, Y. Kamei, T. Todo, T. Ishikawa-Fujiwara, K. Ohno, T. Usami, Y. Nagahama, K. Okubo, Estrogen receptor 2b is the major determinant of sex-typical mating behavior and sexual preference in medaka. *Curr. Biol.* **31**, 1699–1710.e6 (2021).
13. L. Yong, Z. Thet, Y. Zhu, Genetic editing of the androgen receptor contributes to impaired male courtship behavior in zebrafish. *J. Exp. Biol.* **220**, 3017–3021 (2017).
14. B. A. Alward, V. A. Laud, C. J. Skalnik, R. A. York, S. A. Juntti, R. D. Fernald, Modular genetic control of social status in a cichlid fish. *Proc. Natl. Acad. Sci. U.S.A.* **117**, 28167–28174 (2020).
15. Y. Ogino, S. Ansai, E. Watanabe, M. Yasugi, Y. Katayama, H. Sakamoto, K. Okamoto, K. Okubo, Y. Yamamoto, I. Hara, T. Yamazaki, A. Kato, Y. Kamei, K. Naruse, K. Ohta, H. Ogino, T. Sakamoto, S. Miyagawa, T. Sato, G. Yamada, M. E. Baker, T. Iguchi, Evolutionary differentiation of androgen receptor is responsible for sexual characteristic development in a teleost fish. *Nat. Commun.* **14**,

1428 (2023).
16. Y. Nishiike, K. Okubo, The decision of male medaka to mate or fight depends on two complementary androgen signaling pathways. *Proc. Natl. Acad. Sci. U.S.A.* **121**, e2316459121 (2024).
17. N. Diotel, T. D. Charlier, C. Lefebvre d'Hellencourt, D. Couret, V. L. Trudeau, J. C. Nicolau, O. Meilhac, O. Kah, E. Pellegrini, Steroid transport, local synthesis, and signaling within the brain: roles in neurogenesis, neuroprotection, and sexual behaviors. *Front. Neurosci.* **12**, 84 (2018).
18. P. M. Forlano, D. L. Deitcher, D. A. Myers, A. H. Bass, Anatomical distribution and cellular basis for high levels of aromatase activity in the brain of teleost fish: aromatase enzyme and mRNA expression identify glia as source. *J. Neurosci.* **21**, 8943–8955 (2001).
19. N. Diotel, Y. Le Page, K. Mouriec, S. K. Tong, E. Pellegrini, C. Vaillant, I. Anglade, F. Brion, F. Pakdel, B. C. Chung, O. Kah, Aromatase in the brain of teleost fish: expression, regulation and putative functions. *Front. Neuroendocrinol.* **31**, 172–192 (2010).
20. A. Takeuchi, K. Okubo, Post-proliferative immature radial glial cells female-specifically express aromatase in the medaka optic tectum. *PLoS One* **8**, e73663 (2013).
21. S. L. E. Hallgren, M. Linderoth, K. H. Olsén, Inhibition of cytochrome p450 brain aromatase reduces two male specific sexual behaviours in the male Endler guppy (*Poecilia reticulata*). *Gen. Comp. Endocrinol.* **147**, 323–328 (2006).
22. L. A. O'Connell, H. A. Hofmann, Social status predicts how sex steroid receptors regulate complex behavior across levels of biological organization. *Endocrinology* **153**, 1341–1351 (2012).
23. L. S. Huffman, L. A. O'Connell, H. A. Hofmann, Aromatase regulates aggression in the African cichlid fish *Astatotilapia burtoni*. *Physiol. Behav.* **112**, 77–83 (2013).
24. C. Jalabert, L. Quintana, P. Pessina, A. Silva, Extra-gonadal steroids modulate non-breeding territorial aggression in weakly electric fish. *Horm. Behav.* **72**, 60–67 (2015).
25. Y. Nagahama, T. Chakraborty, B. Paul-Prasanth, K. Ohta, M. Nakamura, Sex determination, gonadal sex differentiation, and plasticity in vertebrate species. *Physiol. Rev.* **101**, 1237–1308 (2021).
26. K. Okubo, A. Takeuchi, R. Chaube, B. Paul-Prasanth, S. Kanda, Y. Oka, Y. Nagahama, Sex differences in aromatase gene expression in the medaka brain. *J. Neuroendocrinol.* **23**, 412–423 (2011).
27. M. Nakamoto, Y. Shibata, K. Ohno, T. Usami, Y. Kamei, Y. Taniguchi, T. Todo, T. Sakamoto, G. Young, P. Swanson, K. Naruse, Y. Nagahama, Ovarian aromatase loss-of-function mutant medaka undergo ovary degeneration and partial female-to-male sex reversal after puberty. *Mol. Cell. Endocrinol.* **460**, 104–122 (2018).
28. Y. Taniguchi, S. Takeda, M. Furutani-Seiki, Y. Kamei, T. Todo, T. Sasado, T. Deguchi, H. Kondoh, J. Mudde, M. Yamazoe, M. Hidaka, H. Mitani, A. Toyoda, Y. Sakaki, R. H. A. Plasterk, E. Cuppen, Generation of medaka gene knockout models by target-selected mutagenesis. *Genome Biol.* **7**, R116 (2006).

29. J. Yamashita, A. Takeuchi, K. Hosono, T. Fleming, Y. Nagahama, K. Okubo, Male-predominant galanin mediates androgen-dependent aggressive chases in medaka. *eLife* **9**, e59470 (2020).
30. X. Zhang, Q. Min, M. Li, X. Liu, M. Li, D. Wang, Mutation of *cyp19a1b* results in sterile males due to efferent duct obstruction in Nile tilapia. *Mol. Reprod. Dev.* **86**, 1224–1235 (2019).
31. T. Hiraki, A. Takeuchi, T. Tsumaki, B. Zempo, S. Kanda, Y. Oka, Y. Nagahama, K. Okubo, Female-specific target sites for both oestrogen and androgen in the teleost brain. *Proc. R. Soc. B* **279**, 5014–5023 (2012).
32. S. Yokoi, T. Okuyama, Y. Kamei, K. Naruse, Y. Taniguchi, S. Ansai, M. Kinoshita, L. J. Young, N. Takemori, T. Kubo, H. Takeuchi, An essential role of the arginine vasotocin system in mate-guarding behaviors in triadic relationships of medaka fish (*Oryzias latipes*). *PLoS Genet.* **11**, e1005009 (2015).
33. J. A. Tripp, I. Salas-Allende, A. Makowski, A. H. Bass, Mating behavioral function of preoptic galanin neurons is shared between fish with alternative male reproductive tactics and tetrapods. *J. Neurosci.* **40**, 1549–1559 (2020).
34. Y. Kawabata, T. Hiraki, A. Takeuchi, K. Okubo, Sex differences in the expression of vasotocin/isotocin, gonadotropin-releasing hormone, and tyrosine and tryptophan hydroxylase family genes in the medaka brain. *Neuroscience* **218**, 65–77 (2012).
35. C. M. Klinge, Estrogen receptor interaction with estrogen response elements. *Nucleic Acids Res.* **29**, 2905–2919 (2001).
36. T. Fleming, M. Tachizawa, Y. Nishiike, A. Koiwa, Y. Homan, K. Okubo, Estrogen-dependent expression and function of secretogranin 2a in female-specific peptidergic neurons. *PNAS Nexus* **2**, pgad413 (2023).
37. K. Shaw, M. Therrien, C. Lu, X. Liu, V. L. Trudeau, Mutation of brain aromatase disrupts spawning behavior and reproductive health in female zebrafish. *Front. Endocrinol.* **14**, 1225199 (2023).
38. T. Hiraki, K. Nakasone, K. Hosono, Y. Kawabata, Y. Nagahama, K. Okubo, Neuropeptide B is female-specifically expressed in the telencephalic and preoptic nuclei of the medaka brain. *Endocrinology* **155**, 1021–1032 (2014).
39. T. Hiraki-Kajiyama, J. Yamashita, K. Yokoyama, Y. Kikuchi, M. Nakajo, D. Miyazoe, Y. Nishiike, K. Ishikawa, K. Hosono, Y. Kawabata-Sakata, S. Ansai, M. Kinoshita, Y. Nagahama, K. Okubo, Neuropeptide B mediates female sexual receptivity in medaka fish, acting in a female-specific but reversible manner. *eLife* **8**, e39495 (2019).
40. E. D. Lephart, A review of brain aromatase cytochrome P450. *Brain Res. Rev.* **22**, 1–26 (1996).
41. B. Gegenhuber, M. V. Wu, R. Bronstein, J. Tollkuhn, Gene regulation by gonadal hormone receptors underlies brain sex differences. *Nature* **606**, 153–159 (2022).
42. S. A. Juntti, J. Tollkuhn, M. V. Wu, E. J. Fraser, T. Soderborg, S. Tan, S.-I. Honda, N. Harada, N. M. Shah, The androgen receptor governs the execution, but not programming, of male sexual and territorial behaviors. *Neuron* **66**, 260–272 (2010).
43. M. Bayley, J. R. Nielsen, E. Baatrup, Guppy sexual behavior as an effect biomarker of estrogen

mimics. *Ecotoxicol. Environ. Saf.* **43**, 68–73 (1999).

44. A. M. Bell, Effects of an endocrine disrupter on courtship and aggressive behaviour of male three-spined stickleback, *Gasterosteus aculeatus*. *Anim. Behav.* **62**, 775–780 (2001).
45. R. Bjerselius, K. Lundstedt-Enkel, H. Olsén, I. Mayer, K. Dimberg, Male goldfish reproductive behaviour and physiology are severely affected by exogenous exposure to 17β-estradiol. *Aquat. Toxicol.* **53**, 139–152 (2001).
46. Y. Oshima, I. J. Kang, M. Kobayashi, K. Nakayama, N. Imada, T. Honjo, Suppression of sexual behavior in male Japanese medaka (*Oryzias latipes*) exposed to 17β-estradiol. *Chemosphere* **50**, 429–436 (2003).
47. D. Martinović, W. T. Hogarth, R. E. Jones, P. W. Sorensen, Environmental estrogens suppress hormones, behavior, and reproductive fitness in male fathead minnows. *Environ. Toxicol. Chem.* **26**, 271–278 (2007).
48. D. Kayo, Y. Oka, S. Kanda, Examination of methods for manipulating serum 17β-Estradiol (E2) levels by analysis of blood E2 concentration in medaka (*Oryzias latipes*). Gen Comp. Endocrinol. **285**, 113272 (2020).
49. A. Munakata, M. Kobayashi, Endocrine control of sexual behavior in teleost fish. *Gen. Comp. Endocrinol.* **165**, 456–468 (2010).
50. N. E. Stacey, Effects of indomethacin and prostaglandins on the spawning behaviour of female goldfish. *Prostaglandins* **12**, 113–126 (1976).
51. M. Kobayashi, N. Stacey, Prostaglandin-induced female spawning behavior in goldfish (*Carassius auratus*) appears independent of ovarian influence. *Horm. Behav.* **27**, 38–55 (1993).
52. S. A. Juntti, A. T. Hilliard, K. R. Kent, A. Kumar, A. Nguyen, M. A. Jimenez, J. L. Loveland, P. Mourrain, R. D. Fernald, A neural basis for control of cichlid female reproductive behavior by prostaglandin F2α. *Curr. Biol.* **26**, 943–949 (2016).
53. T. Kimchi, J. Xu, C. Dulac, A functional circuit underlying male sexual behaviour in the female mouse brain. *Nature* **448**, 1009–1014 (2007).
54. B. M. Nugent, C. L. Wright, A. C. Shetty, G. E. Hodes, K. M. Lenz, A. Mahurkar, S. J. Russo, S. E. Devine, M. M. McCarthy, Brain feminization requires active repression of masculinization via DNA methylation. *Nat. Neurosci.* **18**, 690–697 (2015).
55. B. Capel, Vertebrate sex determination: evolutionary plasticity of a fundamental switch. *Nat. Rev. Genet.* **18**, 675–689 (2017).
56. H. Liu, E. V. Todd, P. M. Lokman, M. S. Lamm, J. R. Godwin, N. J. Gemmell, Sexual plasticity: a fishy tale. *Mol. Reprod. Dev.* **84**, 171–194 (2017).
57. H. J. Kim, H. J. Lee, H. Kim, S. W. Cho, J.-S. Kim, Targeted genome editing in human cells with zinc finger nucleases constructed via modular assembly. *Genome Res.* **19**, 1279–1288 (2009).
58. S. G. Lynn, W. J. Birge, B. S. Shepherd, Molecular characterization and sex-specific tissue expression of estrogen receptor α (*esr1*), estrogen receptor βa (*esr2a*) and ovarian aromatase (*cyp19a1a*) in yellow perch (*Perca flavescens*). *Comp. Biochem. Physiol. B Biochem. Mol. Biol.*

149, 126–147 (2008).

59. D. Kayo, B. Zempo, S. Tomihara, Y. Oka, S. Kanda, Gene knockout analysis reveals essentiality of estrogen receptor β1 (Esr2a) for female reproduction in medaka. *Sci. Rep.* **9**, 8868 (2019).
60. Y. Kawabata-Sakata, Y. Nishiike, T. Fleming, Y. Kikuchi, K. Okubo, Androgen-dependent sexual dimorphism in pituitary tryptophan hydroxylase expression: relevance to sex differences in pituitary hormones. *Proc. R. Soc. B* **287**, 20200713 (2020).
61. R. Anken, F. Bourrat, *Brain Atlas of the Medaka fish* (INRA Editions, 1998).
62. Y. Ishikawa, M. Yoshimoto, H. Ito, A brain atlas of a wild-type inbred strain of the medaka, *Oryzias latipes*. *Fish Biol. J. Medaka* **10**, 1–26 (1999).
63. J. H. Kim, S. R. Lee, L. H. Li, H. J. Park, J. H. Park, K. Y. Lee, M. K. Kim, B. A. Shin, S. Y. Choi, High cleavage efficiency of a 2A peptide derived from porcine teschovirus-1 in human cell lines, zebrafish and mice. *PLoS One* **6**, e18556 (2011).
64. O. Yamanaka, R. Takeuchi, UMATracker: an intuitive image-based tracking platform. *J. Exp. Biol.* **221**, jeb182469 (2018).

Figures

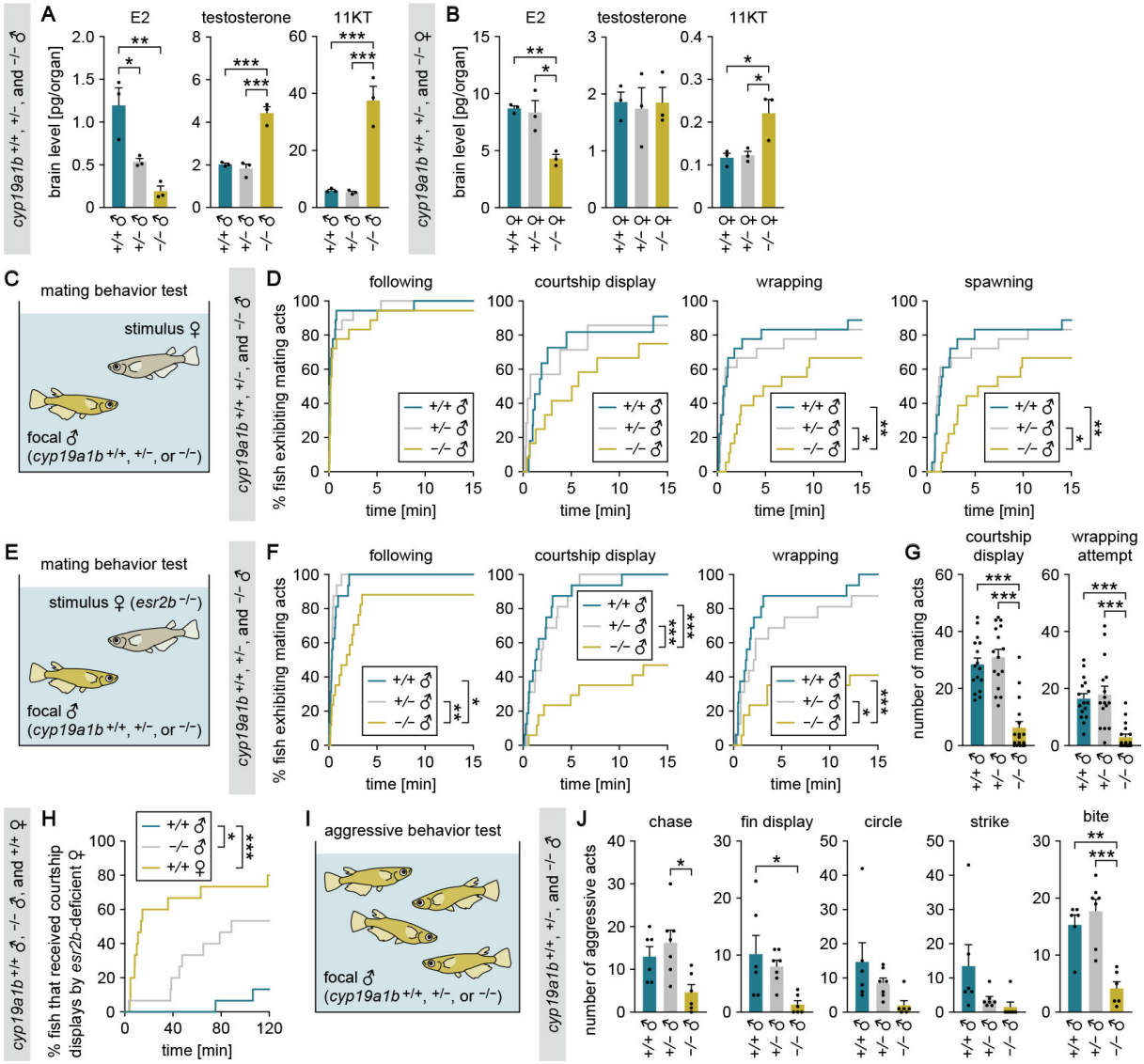

Fig. 1 *cyp19a1b*-deficient males exhibit severely impaired male-typical mating and aggressive behaviors.

(**A** and **B**) Levels of E2, testosterone, and 11KT in the brain of adult *cyp19a1b*$^{+/+}$, *cyp19a1b*$^{+/-}$, and *cyp19a1b*$^{-/-}$ males (A) and females (B) (n = 3 per genotype and sex). (**C**) Set-up for testing the mating behavior of *cyp19a1b*$^{+/+}$, *cyp19a1b*$^{+/-}$, and *cyp19a1b*$^{-/-}$ males. (**D**) Latency of *cyp19a1b*$^{+/+}$, *cyp19a1b*$^{+/-}$, and *cyp19a1b*$^{-/-}$ males (n = 18 per genotype) to initiate each mating act toward the stimulus female. (**E**) Set-up for testing mating behavior using an *esr2b*-deficient female as the stimulus. (**F**) Latency of *cyp19a1b*$^{+/+}$, *cyp19a1b*$^{+/-}$, and *cyp19a1b*$^{-/-}$ males (n = 16, 15, and 17, respectively) to initiate each mating act toward the *esr2b*-deficient female. (**G**) Number of each mating act performed. (**H**) Latency of *cyp19a1b*$^{+/+}$ and *cyp19a1b*$^{-/-}$ males and *cyp19a1b*$^{+/+}$ females (n = 15 each) to receive courtship displays from the *esr2b*-deficient female. (**I**) Set-up for testing aggressive behavior among grouped males. (**J**) Total number of each aggressive act observed among *cyp19a1b*$^{+/+}$, *cyp19a1b*$^{+/-}$, or

824 *cyp19a1b*$^{-/-}$ males in the tank (n = 6, 7, and 5, respectively). Statistical differences were assessed by
825 Bonferroni's or Dunn's post hoc test (A, B, G, and J) and Gehan-Breslow-Wilcoxon test with
826 Bonferroni's correction (D, F, and H). Error bars represent SEM. *$P < 0.05$, **$P < 0.01$, ***$P < 0.001$.

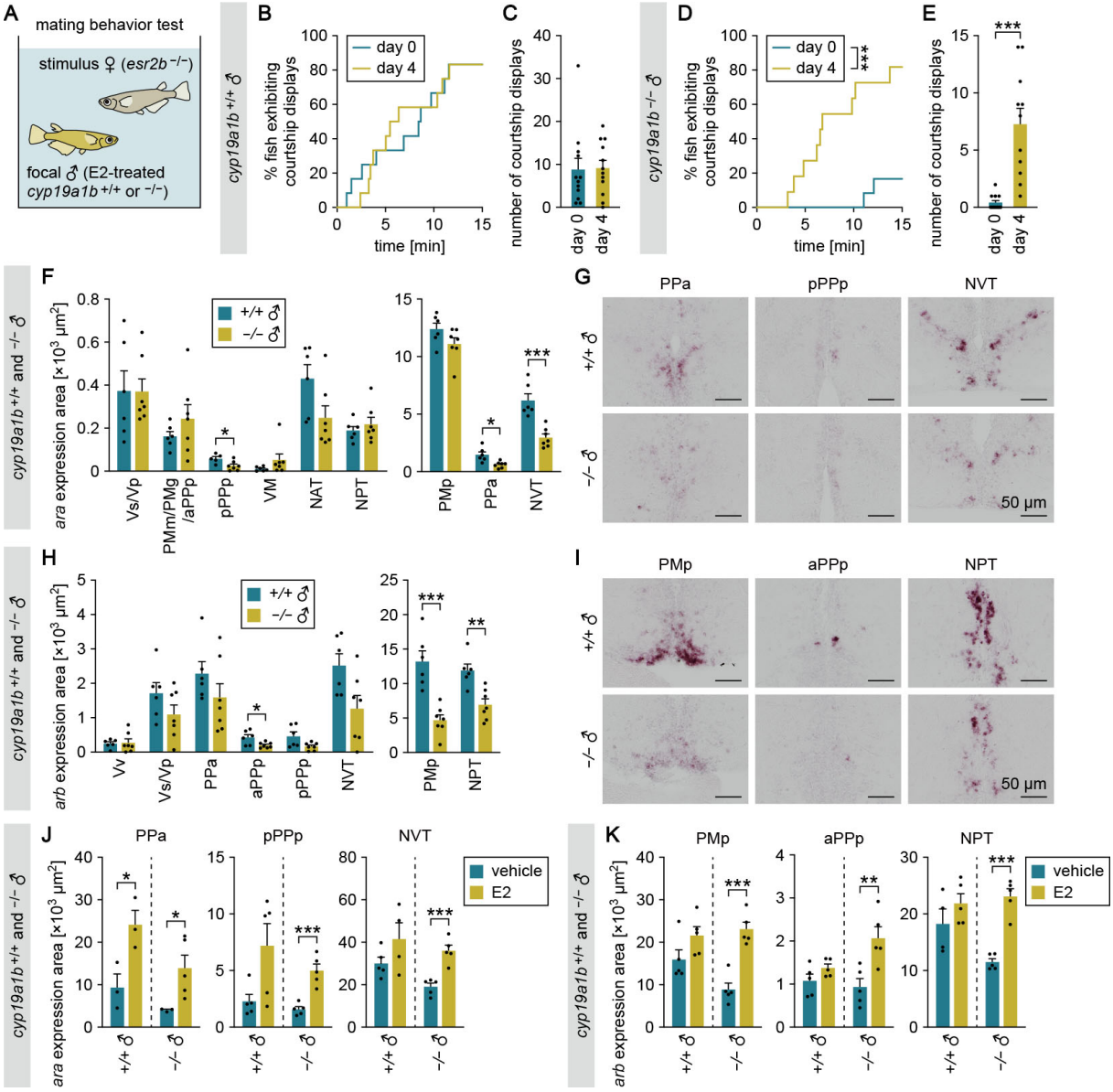

Fig. 2 Brain-derived estrogens facilitate male-typical behaviors probably by stimulating brain AR expression.

(**A**) Set-up for testing the mating behavior of E2-treated *cyp19a1b*$^{+/+}$ and *cyp19a1b*$^{-/-}$ males. (**B**) Latency of *cyp19a1b*$^{+/+}$ males (n = 12) to initiate courtship displays toward the stimulus female before (day 0) and after (day 4) E2 treatment. (**C**) Number of courtship displays performed by *cyp19a1b*$^{+/+}$ males. (**D**) Latency of *cyp19a1b*$^{-/-}$ males (n = 12) to initiate courtship displays before (day 0) and after (day 4) E2 treatment. (**E**) Number of courtship displays performed by *cyp19a1b*$^{-/-}$ males. (**F**) Total area of *ara* expression signal in each brain nucleus of *cyp19a1b*$^{+/+}$ (n = 6 except for pPPp, where n = 5) and *cyp19a1b*$^{-/-}$ (n = 7) males. The data are displayed in two graphs for visual clarity. (**G**) Representative images of *ara* expression in the PPa, pPPp, and NVT. (**H**) Total area of *arb* expression signal in each brain nucleus of *cyp19a1b*$^{+/+}$ (n = 6) and *cyp19a1b*$^{-/-}$ (n = 7 except for NVT, where n = 6) males. The data are displayed in two graphs for visual clarity. (**I**) Representative images of *arb* expression in the PMp, aPPp, and NPT. (**J**) Total area of *ara* expression signal in the PPa, pPPp, and NVT of *cyp19a1b*$^{+/+}$

842 and *cyp19a1b*$^{-/-}$ males treated with vehicle alone or E2 (n = 5 per group except for NVT of E2-treated
843 *cyp19a1b*$^{+/+}$ males, where n = 4; and PPa of vehicle-treated *cyp19a1b*$^{+/+}$, E2-treated *cyp19a1b*$^{+/+}$, and
844 vehicle-treated *cyp19a1b*$^{-/-}$ males, where n = 3). (**K**) Total area of *arb* expression signal in the PMp,
845 aPPp, and NPT of *cyp19a1b*$^{+/+}$ and *cyp19a1b*$^{-/-}$ males treated with vehicle alone or E2 (n = 5 per group
846 except for NPT of vehicle-treated *cyp19a1b*$^{+/+}$ males, where n = 4). Scale bars represent 50 μm. For
847 abbreviations of brain nuclei, see Table S1. Statistical differences were assessed by Gehan-Breslow-
848 Wilcoxon test (B and D) and unpaired *t* test, with Welch's correction where appropriate (C, E, F, H, J,
849 and K). Error bars represent SEM. *$P < 0.05$, **$P < 0.01$, ***$P < 0.001$.

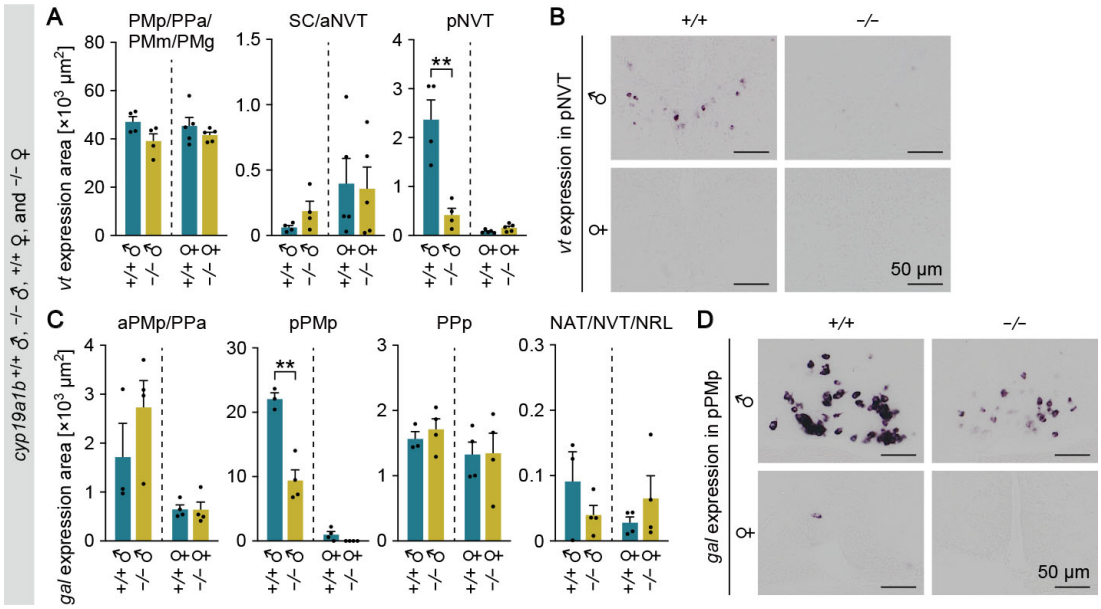

Fig. 3 *cyp19a1b* deficiency impairs behaviorally relevant signaling pathways downstream of ARs.

(**A**) Total area of *vt* expression signal in the PMp/PPa/PMm/PMg, SC/aNVT, and pNVT of $cyp19a1b^{+/+}$ and $cyp19a1b^{-/-}$ males and females (n = 4 and 5 per genotype for males and females, respectively). (**B**) Representative images of *vt* expression in the pNVT. (**C**) Total area of *gal* expression signal in the aPMp/PPa, pPMp, PPp, and NAT/NVT/NRL of $cyp19a1b^{+/+}$ and $cyp19a1b^{-/-}$ males and females (n = 4 except for $cyp19a1b^{+/+}$ males, where n = 3). (**D**) Representative images of *gal* expression in the pPMp. Scale bars represent 50 µm. For abbreviations of brain nuclei, see Table S1. Statistical differences were assessed by unpaired *t* test, with Welch's correction where appropriate (A and C). Error bars represent SEM. $^{**}P < 0.01$.

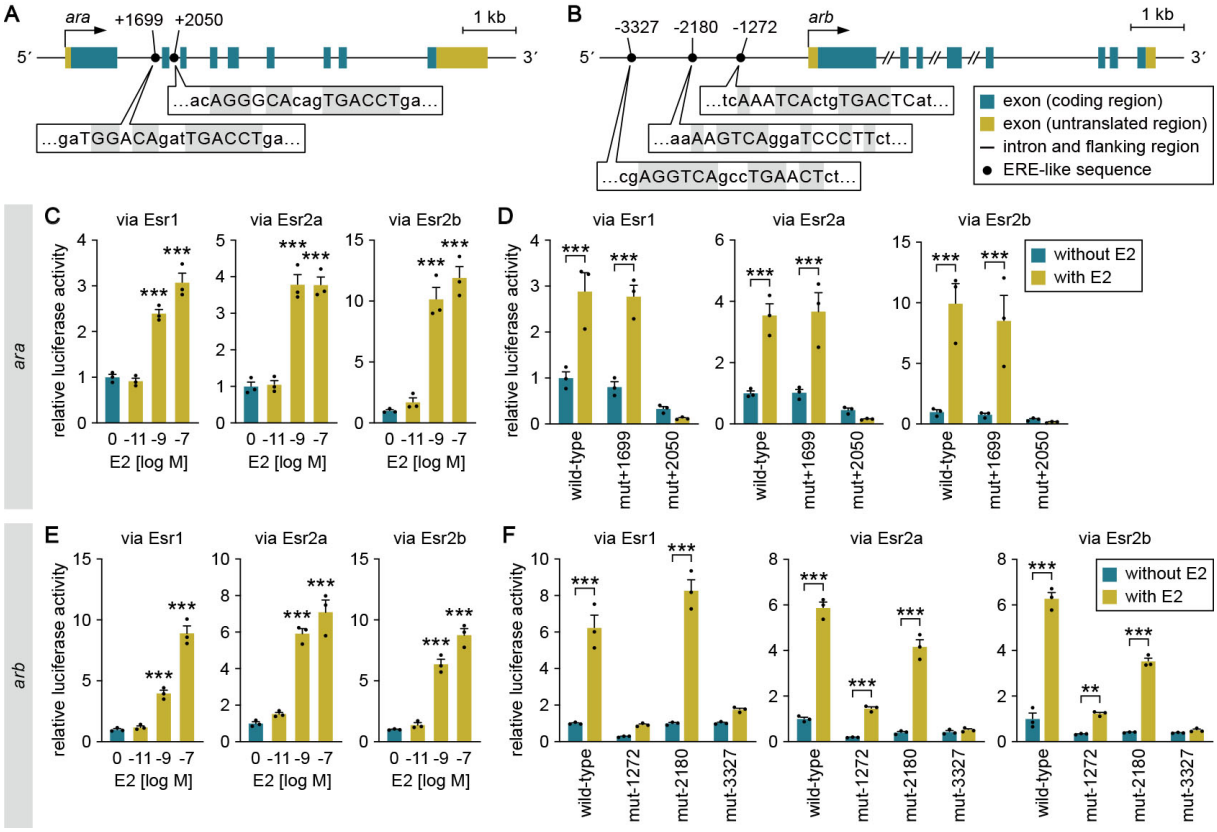

Fig. 4 Estrogens directly stimulate the transcription of ARs through ESRs.

(**A** and **B**) Schematic of *ara* (A) and *arb* (B) loci showing the location of the canonical bipartite ERE-like sequences. Bent arrows mark the transcription initiation sites. Nucleotides of the ERE-like sequences are denoted by capital letters, and those identical to the consensus ERE (AGGTCAnnnTGACCT) are gray-shaded. (**C**) Ability of E2 to directly activate *ara* transcription. Cultured cells were transfected with a luciferase reporter construct containing a genomic fragment upstream of exon 3 of *ara*, together with an Esr1, Esr2a, or Esr2b expression construct. The cells were stimulated with different concentrations of E2 and luciferase activity was measured. (**D**) Effect of mutations in the ERE-like sequences on the E2-induced activation of *ara* transcription. Cultured cells were transfected with a wild-type luciferase construct or a construct carrying a mutation in the ERE-like sequence at position +1699 (mut+1699) or +2050 (mut+2050), together with an Esr1, Esr2a, or Esr2b expression construct. The cells were stimulated with or without E2, and luciferase activity was measured. (**E**) Ability of E2 to directly activate *arb* transcription. The assay described in C was performed with a luciferase construct containing a genomic fragment upstream of the first methionine codon of *arb*. (**F**) Effect of mutations in the ERE-like sequences on the E2-induced activation of *arb* transcription. The assay described in D was performed with luciferase constructs each carrying a mutation in the ERE-like sequence at position –1272 (mut-1272), –2180 (mut-2180), or –3327 (mut-3327). Values are expressed as a fold change relative to a control without E2 stimulation (C and E) or a control using the wild-type construct without E2 stimulation (D and F). Statistical differences were assessed by Dunnett's post hoc test (C and E) and unpaired *t* test with Bonferroni–Dunn correction (D and F). Error bars represent SEM.

884 $^{**}P < 0.01$; $^{***}P < 0.001$.

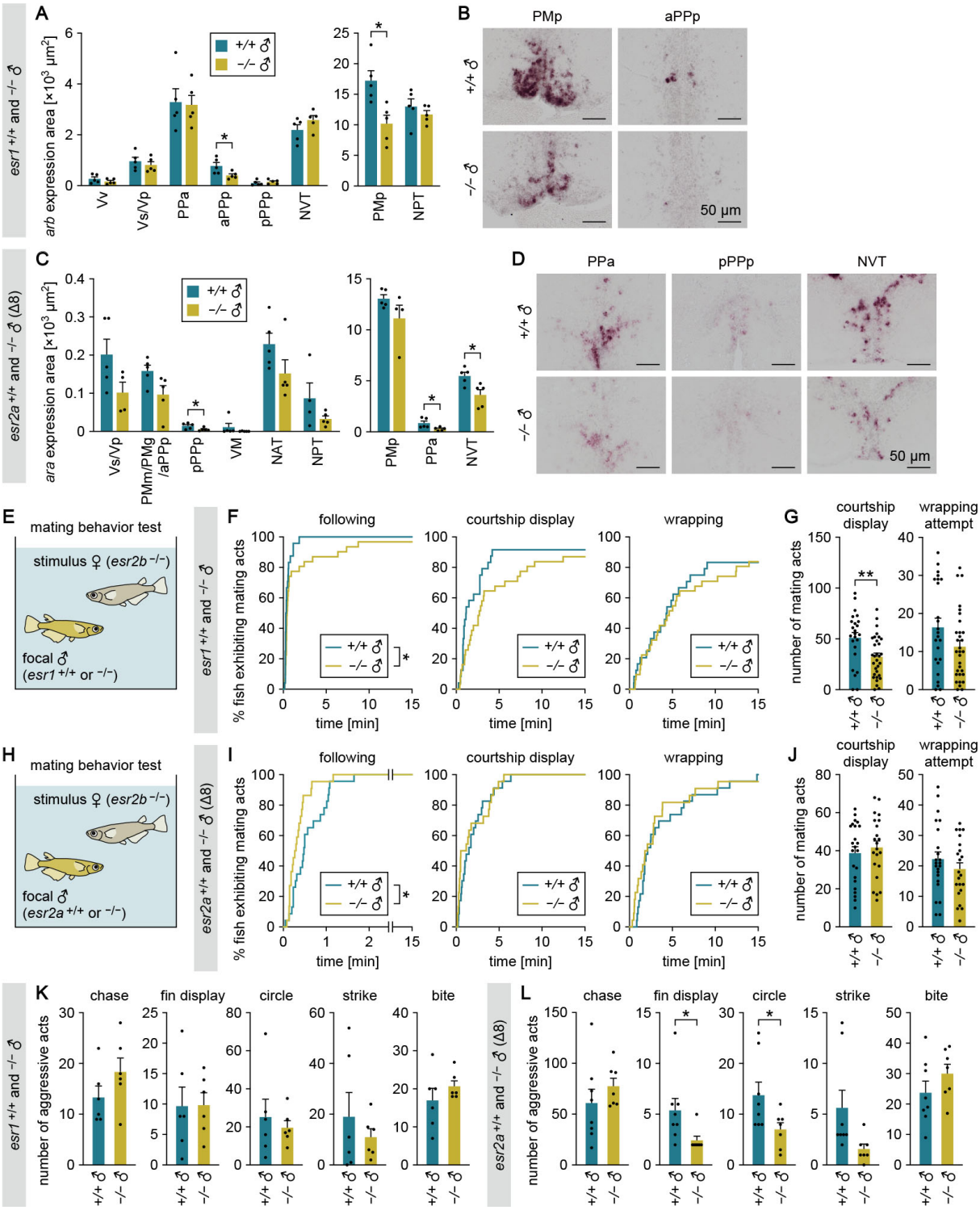

885
886
887 **Fig. 5 Brain-derived estrogens stimulate *ara* and *arb* expression in behaviorally**
888 **relevant brain regions primarily through Esr2a and Esr1, respectively.**
889 (**A**) Total area of *arb* expression signal in each brain nucleus of $esr1^{+/+}$ and $esr1^{-/-}$ males (n = 5 per
890 genotype). The data are displayed in two graphs for visual clarity. (**B**) Representative images of *arb*
891 expression in the PMp and aPPp. (**C**) Total area of *ara* expression signal in each brain nucleus of $esr2a^{+/+}$
892 and $esr2a^{-/-}$ males (Δ8 line; n = 5 per genotype except for NPT of $esr2a^{+/+}$ males and Vs/Vp and PMp

893 of *esr2a*$^{-/-}$ males, where n = 4). The data are displayed in two graphs for visual clarity. (**D**)
894 Representative images of *ara* expression in the PPa, pPPp, and NVT. (**E**) Set-up for testing the mating
895 behavior of *esr1*$^{+/+}$ and *esr1*$^{-/-}$ males using an *esr2b*-deficient female as the stimulus. (**F**) Latency of
896 *esr1*$^{+/+}$ and *esr1*$^{-/-}$ males (n = 24 and 31, respectively) to initiate each mating act toward the stimulus
897 female. (**G**) Number of each mating act performed. (**H**) Set-up for testing the mating behavior of *esr2a*$^{+/+}$
898 and *esr2a*$^{-/-}$ males using an *esr2b*-deficient female as the stimulus. (**I**) Latency of *esr2a*$^{+/+}$ and *esr2a*$^{-/-}$
899 males (Δ8 line; n = 23 and 22, respectively) to initiate each mating act toward the stimulus female. (**J**)
900 Number of each mating act performed. (**K** and **L**) Total number of each aggressive act observed among
901 *esr1*$^{+/+}$ or *esr1*$^{-/-}$ males (n = 6 per genotype) (K) and among *esr2a*$^{+/+}$ or *esr2a*$^{-/-}$ males (Δ8 line; n = 8
902 and 7, respectively) (L) in the tank. Scale bars represent 50 μm. For abbreviations of brain nuclei, see
903 Table S1. Statistical differences were assessed by unpaired *t* test, with Welch's correction where
904 appropriate (A, C, G, J, K, and L) and Gehan-Breslow-Wilcoxon test (F and I). Error bars represent
905 SEM. *$P < 0.05$, **$P < 0.01$.

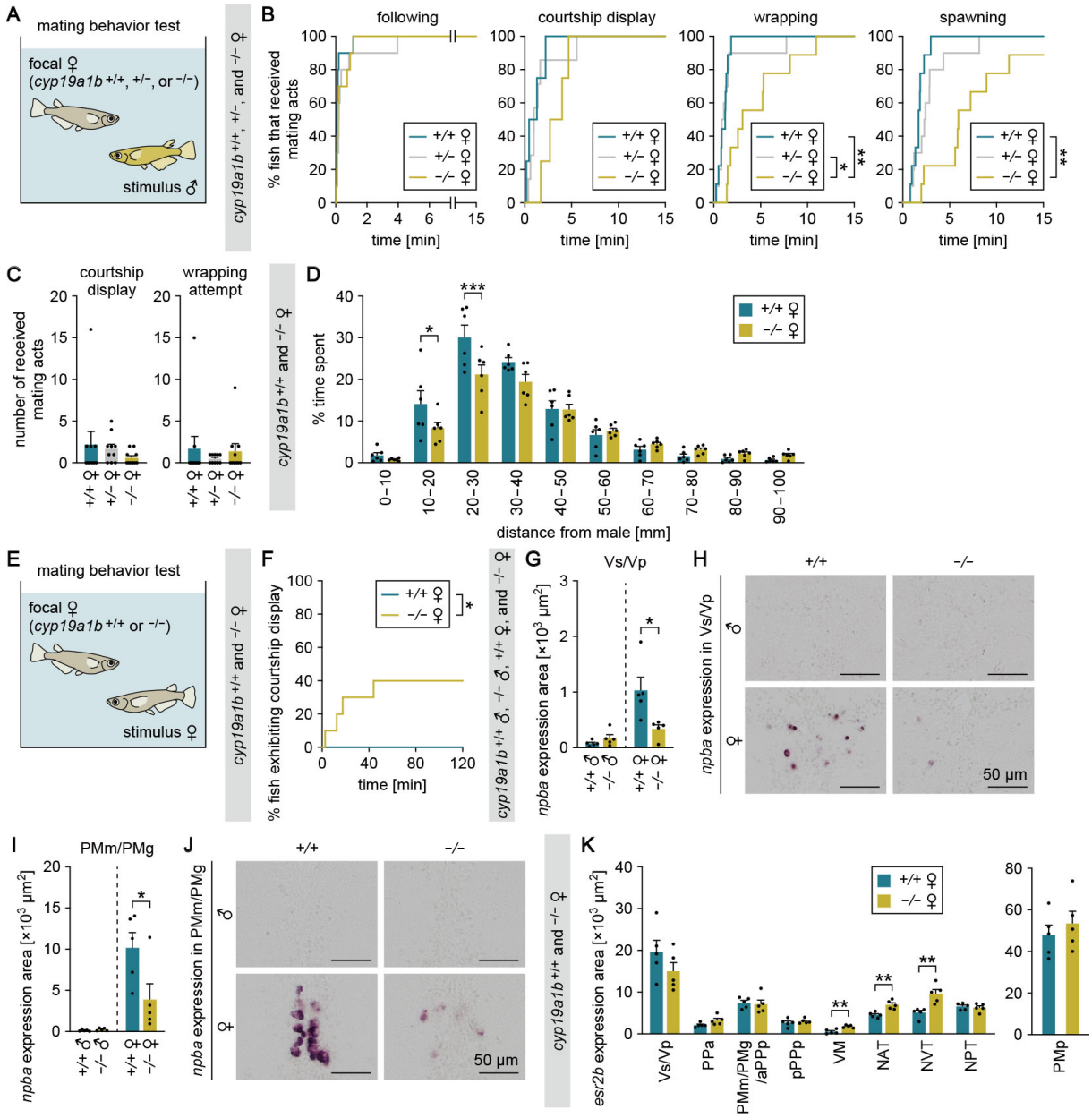

Fig. 6 *cyp19a1b*-deficient females are less receptive to males and instead court other females.

(**A**) Set-up for testing the mating behavior of *cyp19a1b*$^{+/+}$, *cyp19a1b*$^{+/-}$, and *cyp19a1b*$^{-/-}$ females. (**B**) Latency of *cyp19a1b*$^{+/+}$, *cyp19a1b*$^{+/-}$, and *cyp19a1b*$^{-/-}$ females (n = 10 per genotype) to receive each mating act from the stimulus male. (**C**) Number of each mating act received. (**D**) Percentage of time *cyp19a1b*$^{+/+}$ and *cyp19a1b*$^{-/-}$ females (n = 6 per genotype) spent at different distances from the stimulus male. (**E**) Set-up for testing the mating behavior of *cyp19a1b*$^{+/+}$ and *cyp19a1b*$^{-/-}$ females toward a stimulus female. (**F**) Latency of *cyp19a1b*$^{+/+}$ (n = 9) or *cyp19a1b*$^{-/-}$ (n = 10) females to initiate courtship displays toward the stimulus female. (**G** and **H**) Total area (G) and representative images (H) of *npba* expression signal in the Vs/Vp of *cyp19a1b*$^{+/+}$ and *cyp19a1b*$^{-/-}$ males and females (n = 5 per genotype and sex). (**I** and **J**) Total area (I) and representative images (J) of *npba* expression signal in the

919 PMm/PMg of *cyp19a1b*$^{+/+}$ and *cyp19a1b*$^{-/-}$ males and females (n = 5 per genotype and sex). (**K**) Total
920 area of *esr2b* expression signal in each brain nucleus of *cyp19a1b*$^{+/+}$ or *cyp19a1b*$^{-/-}$ females (n = 5 per
921 genotype). The data are displayed in two graphs for visual clarity. Scale bars represent 50 μm. For
922 abbreviations of brain nuclei, see Table S1. Statistical differences were assessed by Gehan-Breslow-
923 Wilcoxon test, with Bonferroni's correction where appropriate (B and F), Bonferroni's post hoc test (C),
924 unpaired *t* test with Bonferroni–Dunn correction (D), and unpaired *t* test, with Welch's correction where
925 appropriate (G, I, and K). Error bars represent SEM. *$P < 0.05$, **$P < 0.01$, ***$P < 0.001$.